Comparison of Frequency Domain Equalizers to Time Domain Equalizers in WCDMA

Yaqoob, Muhammad Atif

2009

Document Version:
Publisher's PDF, also known as Version of record

Comparison of Frequency Domain Equalizers to Time Domain Equalizers in WCDMA

Master Thesis

Muhammad Atif Yaqoob

December 2009

Dedicated to

My Parents

Preface

This thesis work is performed to fulfill the requirements of Master of Science degree. All of the thesis work has been carried out over a period of about 6 months from 01-Jun-09 to 18-Dec-09 at system simulations group EAB/KMT/BDS, ST-Ericsson, Lund and is equivalent to 30 ECTS points. This thesis work is supervised by Elias Jonsson from ST-Ericsson and Fredrik Tufvesson from department of Electrical and Information Technology, LTH, Sweden.

I would like to take this opportunity to express my gratitude to Fredrik Tufvesson who has shown very kind support and guidance as my masters program coordinator at LTH as well as my thesis supervisor. I would like to extend my special thanks to Elias Jonsson for all the technical support and encouragement throughout the period of my thesis work at ST-Ericsson. He remained very kind and supportive during all the time. The frequent discussions I had with him to understand different technical details of the thesis helped me achieve my set objectives timely and effectively. I am also thankful to him for his valuable comments and suggestions for writing this thesis report. Also, I would like to thank my Development Manager Anders Ericsson G for providing me the opportunity to pursue a master thesis in his group.

Finally, I would like to thank to all my friends for their enduring support and encouragement. And to my family for their unconditional love and support during all the time I was involved with my studies. Without their support and encouragement, this work would not be possible.

Abstract

Future mobile platforms will contain an increased amount of wireless technologies. As technologies mature it will be necessary to find synergies between them. This could be in the form of reusing hardware blocks and algorithms. By using Fast Fourier Transforms (FFT/IFFT) and performing channel cancellation/equalization in frequency domain for wideband code division multiple access (WCDMA) will provide us a platform which can support LTE and WiFi together with WCDMA. In this thesis, an equalizer based on Fast Fourier Transforming (FFT) the input signal, cancelling the propagation channel in frequency domain, and finally reverting to time domain using an IFFT would be devised for WCDMA. The performance of frequency domain equalizer is then compared with traditional time domain equalizer based on G-RAKE method for different performance metrics.

To evaluate and compare the performance of frequency domain equalizer (FFT) with time domain equalizer (G-RAKE), a simulator is made in IT++. Several simulations are performed and the obtained results are analyzed in Matlab. Firstly, for channel estimation at the receiver, common pilot channel (CPICH) is used and multiple channel estimates are obtained to get a filtered channel estimate. Along-with CPICH pilot symbols, data symbols of a desired user and four other user's data symbols are transmitted from the base-station (Node B). Using QPSK signaling, un-coded bit-error-rate (BER) results of the desired data user are compared for the two equalization methods. Simulation results are obtained for single path and multi-path propagation channels with different delay spread values. Included in the modeling are one receive and transmit antenna, other cell interference, i.e., non-white noise, frequency errors at mobile station (UE), and analog-to-digital (A/D) quantization.

Table of Contents

Preface ..... **iii**

Abstract ..... **iv**

Table of Contents ..... **v**

List of Figures ..... **viii**

List of Tables ..... **ix**

List of Abbreviations ..... **x**

1 Introduction to Project **1**

1.1 Background 1

1.2 Motivation 1

1.3 Previous Work 1

1.4 Problem Statement 2

1.5 Contribution 2

2 WCDMA Overview **4**

2.1 WCDMA: An Air Interface for UMTS 4

2.2 UMTS System Requirements 4

2.3 WCDMA: Main System Parameters 5

2.4 Time Units 5

2.5 Channels 5

2.6 Spreading and modulation 6

2.6.1 Channelization code 6

2.6.2 Scrambling code 8

2.6.3 Spreading and Transmission over the Air 9

2.7 Common Pilot Channel (CPICH) 11

2.8 Example Using WCDMA 12

2.8.1 Propagation Channel Delay Time Estimation 13

2.8.2 Detection of Propagation Channel Constant 14

2.8.3 Data Demodulation of the Sent Data 14

2.8.3.1 RAKE 15

2.8.3.2 Channel Estimation 16

2.8.3.3 Interference Estimation 16

2.8.3.4 Signal-to-Interference Ratio (SIR) 16

2.8.3.5 Combiner 17

3 Equalizer Model **18**

3.1 Communication System Diagram 18
3.2 RAKE (Time domain) 18
3.2.1 Non-parametric MMSE-based Equalization 19
3.2.2 ML-based Equalization (Non-parametric G-RAKE) 20
3.2.3 SIR 22
3.3 FFT (Frequency domain) 23
3.3.1 System Model 23
3.3.2 Demodulation 24
3.3.3 Approximations to investigate 26
3.3.4 Interference Calculation 26
3.3.5 Power Calculation 27
3.3.6 Calculation of Filtered Channel Estimate 27
Chapter 4 28
4 Implementation and Results 28
4.1 Simulation Setup 28
4.1.1 Transmit Signal from Node B 29
4.1.2 Propagation Channel 31
4.1.3 Signal Reception at UE 31
4.2 GRAKE Equalizer Receiver 33
4.2.1 Channel Estimation 33
4.2.2 Equalizer Filter and SIR 34
4.2.3 Combiner 35
4.3 FFT Equalizer Receiver 37
4.3.1 Channel Estimation 37
4.3.2 Equalizer 38
4.3.3 Despreader Output, BER, and SIR Estimate 39
4.4 Results and Discussion 41
4.4.1 Parameters Optimization 41
4.4.1.1 GRAKE Parameters Optimization 41
4.4.1.2 FFT Parameters Optimization 41
4.4.2 Chip Offset Comparison 44
4.4.3 Frequency Error Comparison 51
4.4.4 Colored Noise Comparison 54
4.4.5 Analog-to-Digital Converter Comparison 55
4.4.6 Complexity Comparison 57
4.4.6.1 FFT Equalizer Output Samples 57
4.4.6.2 Computations For FFT 58
4.4.6.3 Computations for NP-GRAKE 59
4.4.7 ITU-Pedestrian B Channel Comparison 61
5 Conclusion 63

Appendix 65

A. Parametric Equalizer 65

B. Differentiate $\|Hg - e\|^2$ w.r.t g 67

References 69

List of Figures

Figure 2.1: OVSF code tree 8

Figure 2.2: Relationship between Spreading and Scrambling 8

Figure 2.3: Multi-path propagation channel 10

Figure 2.4: Frame structure and modulation pattern for Common Pilot Channel 11

Figure 2.5: Propagation channel estimates 14

Figure 2.6: Data Demodulation Using RAKE 15

Figure 2.7: RAKE Receiver Block Diagram 17

Figure 3.1: Communication System Block Diagram 18

Figure 3.2: FFT Equalizer Receiver Block Diagram 24

Figure 4.1: Root Raised Cosine Filter; sample rate = 4 per chip, filter length = 14chips 29

Figure 4.2: Transmission of WCDMA signal from Node B 30

Figure 4.3: Received Signal at UE via Matched Filtering 32

Figure 4.4: Non-Parametric G-RAKE Receiver Channel Estimation 33

Figure 4.5: Non-Parametric G-RAKE Equalizer Filter and SIR 35

Figure 4.6: Non-Parametric G-RAKE Combiner Output and BER 36

Figure 4.7: FFT Receiver Channel Estimation 37

Figure 4.8: FFT Equalizer Input/Output Block Diagram 39

Figure 4.9: FFT Despreader Output, BER, and SIR Estimate 40

Figure 4.10: FFT Equalizer Output Chip Samples vs Delay Spread 57

Figure 4.11: BER vs EcIor for FFT and GRAKE equalizer using 61

List of Tables

Table 2.1: Main WCDMA parameters 5

Table 2.2: WCDMA Downlink Data Rate vs Spreading Factor 7

Table 4.1: Simulation setup: different users/channels with their *sf* and power assigned 28

Table 4.2: N_{FFT} vs BER for two path channel, 'ds' = 5 chip, λ_h = 1/200, without AWGN 43

Table 4.3: FFT Equalizer BER results for different delay spread values, N_{FFT} = 2048, without AWGN, λ_h = 1/200, ... 44

Table 4.4: Chip Offset Comparison: Single Path Channel 45

Table 4.5: FFT equalizer BER vs ε, IorIoc = 6 dB, two path channel 'ds' = 0.75 chip 46

Table 4.6: Chip Offset Comparison: Two Path Channel 'ds' = 0.75 Chip 47

Table 4.7: FFT equalizer BER results at different offset positions using IorIoc = 8 dB 47

Table 4.8: Chip Offset Comparison: Two Path Channel 'ds' = 1 Chip 48

Table 4.9: Chip Offset Comparison: Two Path Channel 'ds' = 4.5 Chip 49

Table 4.10: Chip Offset Comparison: Two Path Channel 'ds' = 5 Chip 50

Table 4.11: Frequency Error Comparison: Single Path Channel, Offset = 0 Chip 51

Table 4.12: Frequency Error Comparison: Single Path Channel, Offset = 1/2 Chip 52

Table 4.13: Frequency Error Comparison: Two Path Channel 'ds' = 5 Chip, Offset = 0 Chip 53

Table 4.14: Colored Noise Comparison 54

Table 4.15: A/D Conversion Comparison: Single Path, Offset = 0 Chip 55

Table 4.16: A/D Conversion Comparison: Single Path, Offset = 1/2 Chip 55

Table 4.17: A/D Conversion Comparison: Two Path 'ds' = 5 Chip, Offset = 0 Chip 56

Table 4.18: Complexity Comparison between FFT and G-RAKE 60

List of Abbreviations

2G	2nd Generation Mobile Systems
3G	3rd Generation Mobile Systems
3GPP	3rd Generation Partnership Project
A/D	Analog-to-Digital Converter
AWGN	Additive White Gaussian Noise
BER	Bit Error Ratio
BLER	Block Error Ratio
BS	Base Station (Node B for UMTS)
CDMA	Code Division Multiple Access
CPICH	Common Pilot Channel
D/A	Digital-to-Analog Converter
DS-CDMA	Direct Sequence - CDMA
EcIor	The chip power transmitted from Node B
EDGE	Enhanced Data Rates for GSM Evolution
ETSI	European Telecommunications Standards Institute
FDD	Frequency Division Duplex
FDE	Frequency Domain Equalization
FFT	Fast Fourier Transform
GPRS	General Packet Radio Service
IFFT	Inverse Fast Fourier Transform
IMT-2000	International Mobile Telecommunication – 2000
ISI	Inter Symbol Interference
ITU	International Telecommunication Union
Ior	The total transmit power from Node B (normalized to one)
Ioc	Other-cell interference (including radio noise)
IorIoc	Amount of inter-cell interference
LOS	Line of sight
MAI	Multiple Access Interference
ML	Maximum Likelihood
MMSE	Minimum Mean Square Error

MRC	Maximum Ratio Combining
MS	Mobile Station (UE for UMTS)
N_{FFT}	FFT window size
NP-GRAKE	Non-parametric Generalized RAKE
PN	Pseudo-Noise
QPSK	Quadrature Phase Shift Keying
RRC	Root Raised Cosine
SIR	Signal to Interference Ratio
UMTS	Universal Mobile Telecommunication System
UE	User Equipment
WCDMA	Wideband Code Division Multiple Access
ds	delay spread
os	over sampling
pdf	probability distribution function
sf	Spreading Factor
w.r.t	with respect to

Chapter 1

1 Introduction to Project

1.1 Background

In today's platforms equalizers that neutralize inter-symbol interference (ISI) from the serving cell as well as other cell interference is becoming a standard feature. Future platforms will contain an increased amount of different wireless technologies. As technologies mature it will be necessary to find synergies between them. This could be in the form of reusing hardware blocks and algorithms. One such example is also shown in [11], where the dedicated hardware blocks are shared and reused by different systems such as DAB, DVB-T, HIPERLAN-2 and UMTS.

1.2 Motivation

In this thesis we will compare an equalizer based on frequency domain equalization (FDE) to traditional time domain method (G-RAKE) for WCDMA in the downlink FDD mode. Frequency domain equalization will be performed by Fast Fourier Transforming (FFT) the input signal, cancelling the influence of propagation channel in frequency domain, and finally reverting to time domain using an IFFT.

Albeit using an FFT for WCDMA equalization might be more computationally expensive than today's time domain methods, however, the total complexity may go down when combined with OFDM based technologies. Using Fast Fourier Transforms (FFT/IFFT) for frequency domain equalization or channel cancellation in WCDMA will provide us a platform which can support LTE and WiFi together with WCDMA.

1.3 Previous Work

Multiple implementation strategies for the frequency domain equalization (FDE) of DS-CDMA signal have been proposed in the literature [12], [13] and [14]. In theses references, the usefulness of FDE over traditional time domain (RAKE) equalization is illustrated by doing channel equalization based on Minimum Mean Square Error (MMSE) criterion to

combat multiple-access interference (MAI) and inter-symbol interference (ISI) and having the same or lesser complexity requirements as well. Also [16] demonstrated that MMSE based equalizer has better BER performance as compared to zero-forcing (ZF) and RAKE equalizer in downlink CDMA.

Moreover, it is proposed that frequency domain equalization combined with single carrier modulation has comparable performance results as of OFDM system having nearly the same complexity requirements [15].

1.4 Problem Statement

The objective with the thesis is to evaluate and compare WCDMA equalizers based on the G-RAKE, and FFT methods for multi-path zero Doppler propagation channels.

Metrics used to evaluate are:

1. Bit error rate for QPSK signaling
2. Sensitivity to frequency errors (the mobile phone (UE) internal clock and the base-station (Node B) clocks are not synchronized; the clocks decide the sampling rate in the A/D converters)
3. Sensitivity to analog to digital (A/D) quantization
4. Number of complex operations required per data symbol

1.5 Contribution

A simulator is made in IT++ to compare the different WCDMA equalizers and to achieve the above mentioned objectives. ML-based G-RAKE method (Non-parametric G-RAKE) is used for time domain equalization and FFT method is used for frequency domain equalization, where FFT window size is selected as 2048. More details about the equalizer models and implementation is provided in chapter 3 and 4.

Simulations are performed to compare an FFT equalizer to G-RAKE equalizer for non-fading or non-time selective propagation channels. Using QPSK signaling for the desired data user, raw bit-error-rate (BER) performance results are compared to evaluate the performance of the two equalizers. Additive White Gaussian Noise (AWGN) is added to the received signal; and the BER performance is compared w.r.t IorIoc values.

By using a tuned parameter *'ε'* which represents the noise variance, simulations are performed to estimate the best expected performance of the FFT based equalizer for various channel conditions. Optimum values of *'ε'* used in the simulations are estimated by observing the un-coded BER performance results. Simulation results are shown in section 4.4 and onwards.

Furthermore, different frequency errors (5, 10, 20 Hz) are generated at the mobile-station (UE) to simulate the synchronization mismatch between the clocks of UE and Node B, and BER performance of the two equalizer methods is compared. Non-white noise, i.e., interference from another Node B is added to the desired signal with appropriate scaling and BER performance results are evaluated using the two equalization methods. Also analog-to-digital quantization results for different (8, 10, and 12-bit) fixed point implementations with appropriate A/D-constant (K) values used to scale the signal for integer representation, are observed. After the simulation results, a basic complexity comparison is made in terms of total complex operations required per data symbol using G-RAKE and FFT method based on the algorithms used for FFT/IFFT and for other matrix operations. Conclusion and possible future work for the FFT based equalization method is given in Chapter 5.

Chapter 2

2 WCDMA Overview

2.1 WCDMA: An Air Interface for UMTS

The success of second-generation (2G) cell phones, especially the Global System for Mobile communications (GSM), motivated the development of a successor system [1]. The 2G systems provided not only voice traffic on mobile phones but also some basic data services, e.g., the short message service (sms). But these data services are limited to use as higher data rates are not available which eventually limits the use of mobile phones for high quality multimedia services.

Under the name of IMT-2000, International Telecommunication Union (ITU) asked for proposals to standardize the work of third-generation (3G) mobile telecommunication systems. A standard has been formulated by 3GPP, which is a joint venture of several standard developing organizations from different regions of the world (Europe, Japan, Korea, USA, and China).

2.2 UMTS System Requirements

The requirements for the third-generation systems are given as under [3]:

- Bit rates up to 2 Mbps;
- Variable bit rate to offer bandwidth on demand;
- Multiplexing of services with different quality requirements on a single connection, e.g. speech, video and packet data;
- Co-existence of second and third generation systems and inter-system handovers for coverage enhancements and load balancing;
- High spectrum efficiency.

2.3 WCDMA: Main System Parameters

In the standardization forums, WCMDA technology has emerged as the most widely adopted third generation air interface. Table 2.1 shows the main system design parameters related to the WCDMA air interface [3]:

Table 2.1: Main WCDMA parameters

• Multiple access method	DS-CDMA
• Duplexing method	Frequency division duplex / time division duplex
• Base station synchronization	Asynchronous operation
• Chip rate	3.84 Mcps
• Frame length	10 ms
• Service multiplexing	Multiple services with different quality of service requirements multiplexed on one connection
• Multirate concept	Variable spreading factor and multicode
• Detection	Coherent using pilot symbols or common pilot
• Multiuser detection, smart antennas	Supported by the standard, optional in the implementation

2.4 Time Units

Transmission Time Interval (TTI): 10, 20, 40, 80 ms, which reflect the different time durations used to transmit coded packets of information.

- Frame: 10 ms
- Slot: 15 slots = 1 frame
- Chip: 38400 chips = 1 frame or 2560 chips = 1slot

2.5 Channels

UMTS uses a number of logical and physical channels. The logical channels in UMTS are of two types: common transport channels and dedicated transport channels. Example of common channels is BCH (broadcast channel), PCH (paging channel), and RACH (random access channel) and are shared by a group of MSs in a cell.

Physical channels are used to carry different control and user information. Information is mapped on to the physical channels for transmission from base station (Node B) to mobile

station (MS) or vice versa. A physical channel that is used for data and control signaling in WCDMA is known as dedicated physical data channel (DPDCH) and is used for both uplink and downlink transmission. Common pilot channel (CPICH) is a downlink physical channel used to transmit known pilot symbols for channel estimation at UE and is discussed in more detail in section 2.5. Details about other different channels used in WCDMA can be found in the standard and also in literature [3], and [4].

2.6 Spreading and modulation

Direct-Sequence code division multiple-access (DS-CDMA) is employed in WCDMA. Different users are assigned different codes (in the form of chips) derived from CDMA. Codes are used to separate different users, and also they distinguish between users and other control channels. Two types of codes: channelization codes and scrambling codes are used to spread the user information and to assign identification tag to the different users. Basic theory about CDMA is described in the references [5], [6], and [7].

2.6.1 Channelization code

Orthogonal channelization codes are used in WCDMA. Let $C^{(n)}$ be a vector of length 4, 8, 16, 32, 64, 128, or 256. The length of the vector is called the spreading factor (sf). And a channelization code is characterized by

$$\sum_{i=1}^{sf} C_i^{(n)}.C_i^{(m)} = \begin{cases} sf, & n = m \\ 0, & n \neq m \end{cases}$$

where each element of $C^{(n)}$ equals ± 1, and $C^{(n)}, C^{(m)}$ are two channelization codes.

Orthogonal variable spreading factor (OVSF) code tree is used in WCDMA to assign the channelization codes to different users. Depending on the user's data rate, code is assigned to the user from the code tree. Where a short code implies high data rate and long code is used for low data rate user. WCDMA downlink data rates (modulation scheme: QPSK) w.r.t the spreading factor used are listed in table 2.2.

Table 2.2: WCDMA Downlink Data Rate vs Spreading Factor

Code length (spreading factor)	WCDMA (Downlink) Data Rate
4	1.92 Mbps
8	960 kbps
16	480 kbps
32	240 kbps
64	120 kbps
128	60 kbps
256	30 kbps
512	15 kbps

An OVSF code tree is shown in figure 2.1. Since a constant chip rate (3.84 Mcps) is used in WCDMA, different data rates are achieved by directly changing the spreading factor. Multiplying the spreading factor by 2 means the data rate is reduced by 2 correspondingly. Spreading factor of 1 can only be used if only one data stream is transmitted, because no other code can be used in this case. Also if parent code e.g. $C_{(4,3)}$ is assigned to one user, then the codes e.g., $C_{(8,5)}$, $C_{(8,6)}$, … from the parent tree can not be assigned to other users at the same time.

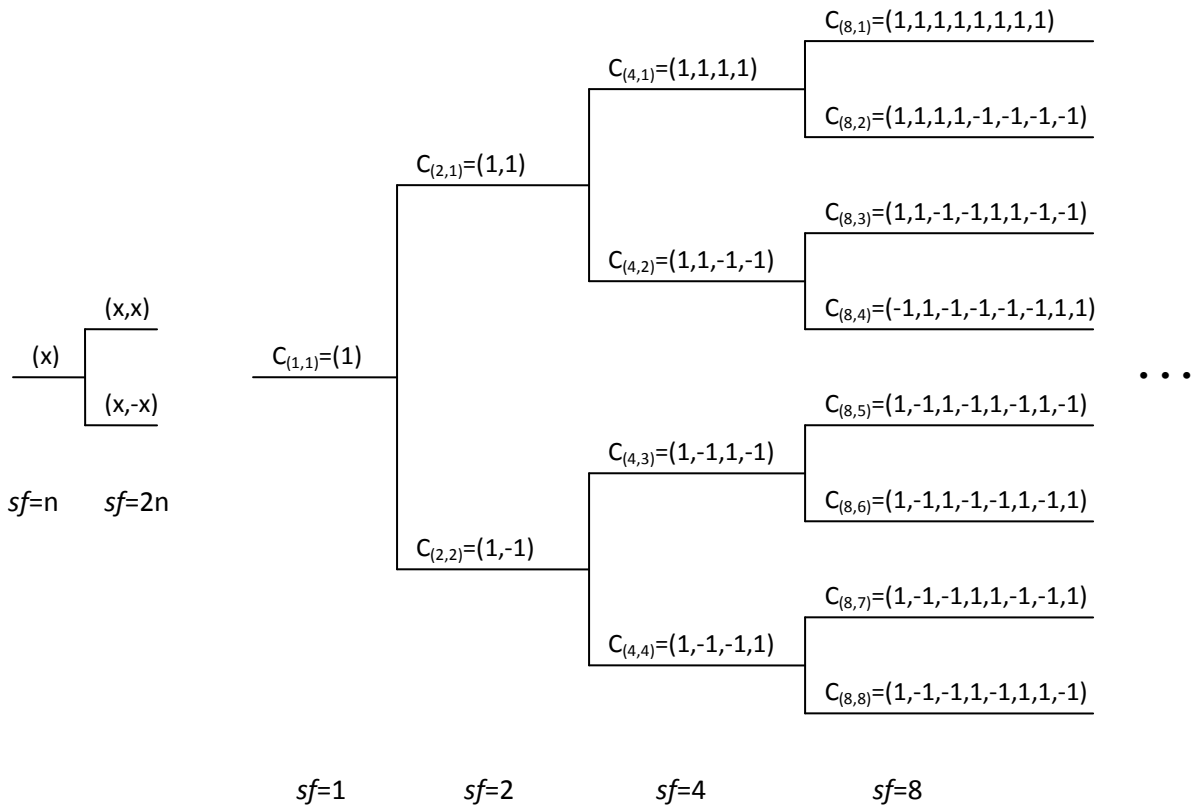

Figure 2.1: OVSF code tree

2.6.2 Scrambling code

Scrambling code is uniquely assigned to different base stations in the network. Also each (UE) has its own scrambling code. It is used as an identification tag; it separates the base stations (in downlink) and UEs (in uplink). Scrambling does not spread any further the chip sequence generated by spreading, but only scramble it by simple multiplication. In figure 2.2, relationship between spreading and scrambling is shown:

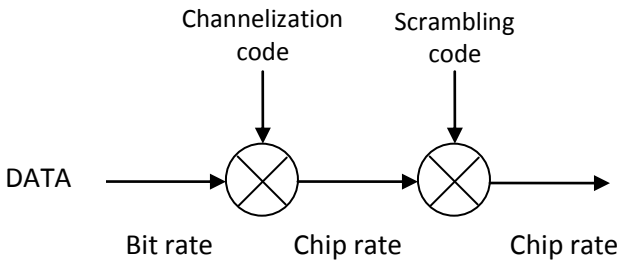

Figure 2.2: Relationship between Spreading and Scrambling

They are quasi-orthogonal random sequences; e.g., a scrambling code is a vector $q^{(n)}$ of length 38400, where each vector entry of $q^{(n)}$ is a complex number of type $(\pm 1 \pm i)/\sqrt{2}$. The scrambling code is constructed to approximate a random sequence, that is,

$$\frac{1}{38400}\sum_{i=0}^{38399} q_i^{(n)} \cdot \left(q_{(i-m) \bmod 38400}^{(n)}\right)^* = \begin{cases} 1, & m = 0 \\ \approx 0, & m \neq 0 \end{cases},$$

observe that if $m \neq 0$ the correlation is not equal to zero, but almost.

2.6.3 Spreading and Transmission over the Air

Let S_n denote the symbols to be sent. Spread the symbols S_n using the channelization code C, that is,

$$S_n \rightarrow S_n C_1, S_n C_2, \ldots, S_n C_{sf},$$

then multiply each spread term with the cell specific scrambling code q,

$$S_n C_1 q_1, S_n C_2 q_2, \ldots, S_n C_{sf} q_{sf},$$

If S_{n+1} is the next symbol to be transmitted, we get similarly, first by spreading

$$S_{n+1} \rightarrow S_{n+1} C_1, S_{n+1} C_2, \ldots, S_{n+1} C_{sf},$$

and afterwards by scrambling

$$\rightarrow S_{n+1} C_1 q_{sf+1}, S_{n+1} C_2 q_{sf+2}, \ldots, S_{n+1} C_{sf} q_{2sf}$$

Observe that the channelization code is reused for each new symbol, but the scrambling code vector continues to be read until we reach the end of it. When the end of the scrambling code has been reached, we start reading it from the beginning.

The purpose of the channelization codes is for the cell to be able to transmit simultaneously several symbols to different UEs.

We have that at any given time a "CHIP" of the type $S_i C_j q_k = X_n$ which needs to be transmitted.

Alternatively, the above operation can be described as:

Symbols $\rightarrow$ Spreading $\rightarrow$ Scrambling $\rightarrow$ Transmit
$\rightarrow$ Propagation Channel Distortion $\rightarrow$ UE-reception

Also, pulse shaping is applied on the generated chips before transmission. In WCDMA, standard root raised cosine (rrc) pulse shape filter is used at the transmitter and matched filter with the same filter is performed at the receiver. More details about the pulse shape filter used is given section 4.1.1.

The sent X_n are affected by the propagation channel. The propagation channel will change the amplitude and phase of the chips.

The received chips at the UE can be modeled as

$$y_n = \sum_{l=1}^{L} h_l \cdot X_{n-\tau(l)} + \nu_n \qquad (2.1)$$

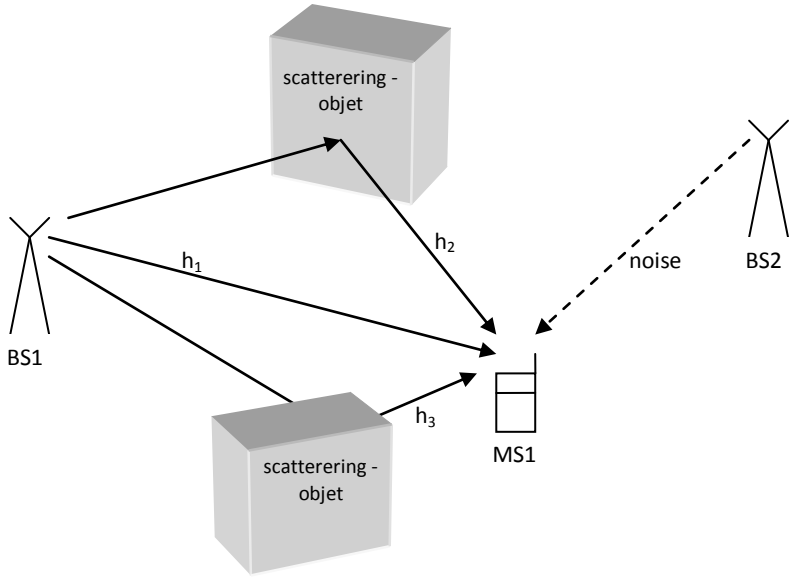

Figure 2.3: Multi-path propagation channel

where $h_{(l)}$ is a complex number modeling path l, and $\tau(l)$ is the time delay between the cell and the UE (time unit in chips) and ν_n is the disturbance (noise) from other cells transmission. Different multi-path signal components arriving at the MS from two different BSs are shown in the above figure 2.5.

2.7 Common Pilot Channel (CPICH)

The CPICH is a fixed rate (30kbps, SF=256) downlink physical channel that carries a pre-defined bit sequence. Figure 2.5 shows the frame structure and modulation pattern of the CPICH. The figure shows that one radio frame having duration of 10ms is composed of 15 slots where each slot carries 2560 chips. 10 CPICH symbols (QPSK modulated of the form 1-i) corresponding to 20 bits are mapped onto these 2560 chips for channel estimation at the UE. In total 38,400 = 2560x15 chips are transmitted in one frame.

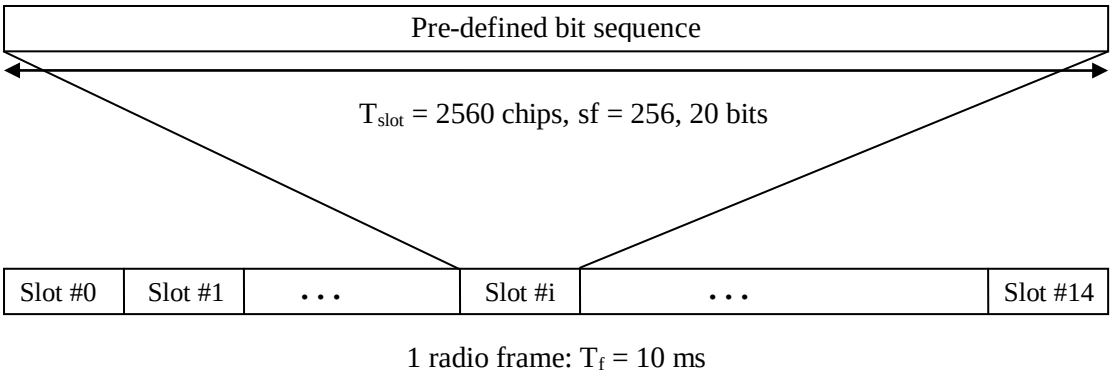

Pre-defined bit sequence of the CPICH (20 bits: all zeros)

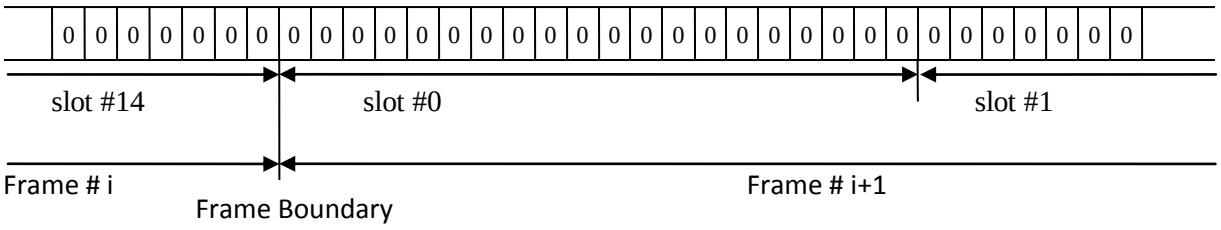

Figure 2.4: Frame structure and modulation pattern for Common Pilot Channel

CPICH symbols $\rightarrow$ Spreading using a 256 chip long channelization code = $C_{(256,1)}$, all ones (1, 1, …, 1) $\rightarrow$ Apply cell specific scrambling code $\rightarrow$ Send over the air

2.8 Example Using WCDMA

Assume an AWGN channel with the following impulse response

$$h_l = \begin{cases} 1, & l = 1 \\ 0, & l = 2,3,4,\cdots \end{cases},$$

Assume that 256 chips are received corresponding to one CPICH symbol. The chips received at the UE can be expressed as

$$y_n = X_n^{(i)}$$

$$+ O_n(\text{other channels or users sent from the same cell using orthogonal channelization codes})$$

$$+ q_n(\text{inter - cell interference, chips received from other BSs})$$

The subscript *'n'* shows the chip index and superscript *'i'* is used for a channelization code. Now if the received signal (y_n) is correlated with the conjugate of $X_n^{(i)}$ and normalized by $1/256$, we have the following expression

$$\frac{1}{256}\sum_{n=0}^{255} y_n.\left(X_n^{(i)}\right)^* = \frac{1}{256}\sum_{n=0}^{255}\underbrace{\left|X_n^{(i)}\right|^2}_{=1}$$

$$+0\left(\begin{array}{c}\textit{other channels use channelization}\\ \textit{codes orthogonal to the CPICH}\end{array}\right)$$

$$+\underbrace{\frac{1}{256}\sum_{n=0}^{255} q_n.\left(X_n^{(i)}\right)^*}_{=\nu}$$

$$\Rightarrow \qquad \frac{1}{256}\sum_{n=0}^{255} y_n.\left(X_n^{(i)}\right)^* = 1+\nu$$

And the expected value of the power is then

$$E\left\{\left|\frac{1}{256}\sum_{n=0}^{255} y_n.\left(X_n^{(i)}\right)^*\right|^2\right\} = E\left\{\left|1+\nu\right|^2\right\}$$

Now

$$E\left\{\left|1+\nu\right|^2\right\}=E\left\{1+\left|\nu\right|^2+2\,\mathrm{Re}(\nu)\right\}$$

Since q_n & $X_n^{(i)}$ are uncorrelated and $E\{q_n\}=E\left\{X_n^{(i)}\right\}=0$, this implies

$$E\left\{\left|1+\nu\right|^2\right\}=1+\frac{1}{256^2}\sum_{n=0}^{255}E\left\{\left|q_n\right|^2\right\}.E\left\{\underbrace{\left|X_n^{(i)}\right|^2}_{=1}\right\}=1+\frac{\sigma^2}{256}$$

where $\sigma^2=E\left\{\left|q_n\right|^2\right\}$ and equals the average power of the inter-cell interference.

2.8.1 Propagation Channel Delay Time Estimation

We will use the CPICH again in our analysis now to detect the time location of the propagation channel paths. The signal received at the UE is given by

$$y_n=\sum_{l=1}^{L}h_l.\left[X_{n-\tau(l)}+other\ \ channels\ \ from\ the\ cell\ \left(O_{n-\tau(l)}\right)\right]$$

$$+\ Inter\text{-}cell\ Interference\ \left(q_n\right) \qquad (2.3)$$

where X_n is the chip sequence containing the CPICH symbols, channelization code, and scrambling code. And (L) represent the number of multi-paths arriving at the MS from Node B.

For different time/chips shifted version of X_n, lets define the correlation of y_n with $\left(X_{n-m}\right)^*$ as follows:

$$Z_m=\sum_{n=0}^{255}y_n.\left(X_{n-m}\right)^*=\sum_{l=1}^{L}\sum_{n=0}^{255}h_l\left(X_{n-\tau(l)}+O_{n-\tau(l)}\right)X_{n-m}^*+q_nX_{n-m}^*$$

The expectation value of Z_m is

$$E\{Z_m\}=\begin{cases}256\,h_l, & m=\tau(l)\ for\ some\ l=1,\ldots,L\\ 0, & m\neq\tau(l)\ for\ some\ l=1,\ldots,L\end{cases} \qquad (2.4)$$

The result follows from the fact that $q_n\,\&\,X_{n-m}^*$ are uncorrelated due to different scrambling codes, $O_n\,\&\,X_{n-m}^*$ are orthogonal if $m=0,$ and uncorrelated if $m\neq0$ due to scrambling code

properties. Similarly $X_n \& X^*_{n-m}$ are uncorrelated if $m \neq 0$ from the scrambling code properties.

Figure 2.6 shows different peaks corresponding to different propagation paths (different values of *m*).

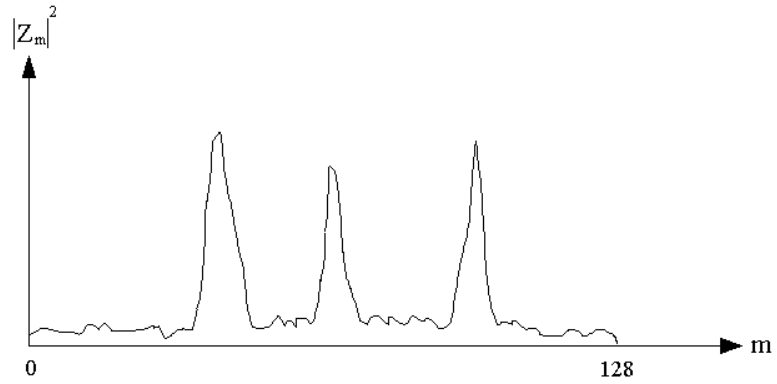

Figure 2.5: Propagation channel estimates

A window, that is, the number of m used, typically spans 64-128 chips. A typical propagation channel has a delay spread of roughly 5 chips.

2.8.2 Detection of Propagation Channel Constant

From the previous section; to find the propagation channel amplitude and phase distortions, the use of CPICH gives us the following result:

$$\frac{1}{256}\sum_{n=0}^{255} y_n . \left(X_{n-\tau(l)}\right)^* \approx h_l$$

where h_l includes the over all channel response (Tx filter + propagation channel + Rx filter).

2.8.3 Data Demodulation of the Sent Data

The received signal is as before

$$y_n = \sum_{l=1}^{L} h_l . \left[X_{n-\tau(l)} + Other\ channels\ \ from\ the\ cell\ \left(O_n\right)\right]$$

$$+\ Inter\text{-}cell\ Interference\ \left(q_n\right)$$

where X_n is n^{th} chip containing the data we want to extract, multiplied by a channelization and scrambling code. To simplify the notation assume data symbol *S* corresponds to chip indexes 1, … , *sf* . We want to extract the symbol *S*.

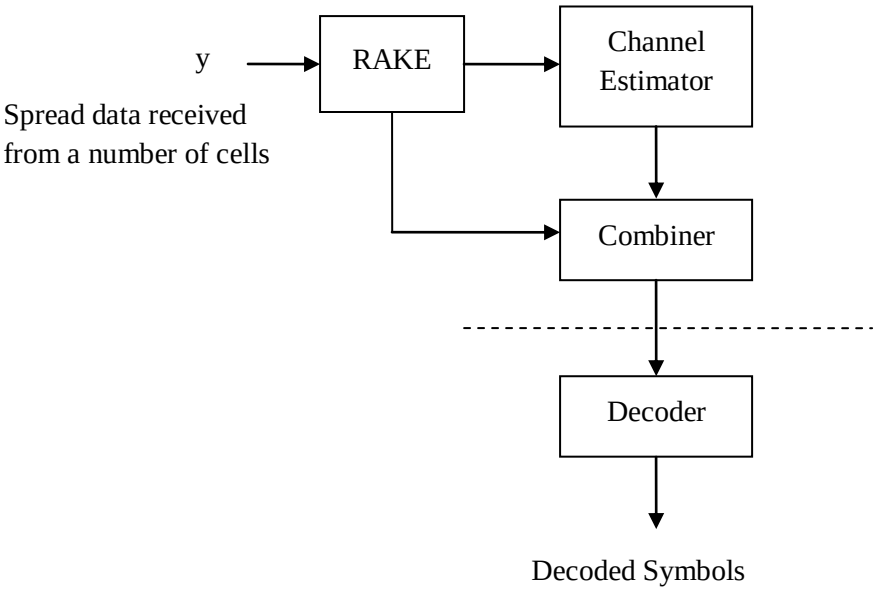

Figure 2.6: Data Demodulation Using RAKE

2.8.3.1 RAKE

The despreading is done in the RAKE, that is, correlate y_n with $\left(\tilde{X}_{n-\tau(l)}\right)^*$, where $\tilde{X}_n$ is the chip sequence formed by the channelization code and scrambling code of the desired user or symbol. Rake outputs are obtained for l paths or braches as described in the following equation and also shown in figure 2.7.

$$r_l = \frac{1}{sf}\sum_{n=0}^{sf-1} y_n . \left(\tilde{X}_{n-\tau(l)}\right)^* \approx h_l S$$

by using the below mentioned results

$$\frac{1}{sf}\sum_{n=0}^{sf-1}\left(\tilde{X}_{n-\tau(l)}\right)^* . X_{m-\tau(l)} = \begin{cases} S, & m = n \\ \approx 0, & m \neq n \end{cases}$$

$$\frac{1}{sf}\sum_{n=0}^{sf-1}\left(\tilde{X}_{n-\tau(l)}\right)^* . (Other\ channels) \approx 0$$

$$\frac{1}{sf}\sum_{n=0}^{sf-1}\left(\tilde{X}_{n-\tau(l)}\right)^* . (Intercell\quad Interference) \approx 0$$

A simple block diagram showing the operations required to extract the sent symbol S is shown in figure 2.8.

2.8.3.2 Channel Estimation

Using the CPICH we can estimate h_l , since the symbol S is then known. In a slot, we have 10 CPICH symbols and consequently we have 10 channel samples per slot, call them

$$h_{l,i}^{samp}, \quad i = 1, \cdots, 10$$

To calculate a channel estimate, use the average of the samples over a slot, that is,

$$h_l^{est} = \frac{1}{10} \sum_{i=1}^{10} h_{l,i}^{samp}$$

Or the channel samples can be filtered by using the following equation:

$$h_{l,i}^{est} = \lambda_h h_{l,i}^{samp} + (1 - \lambda_h) h_{l,i-1}^{est}, \qquad i = 1, \cdots, 10$$

2.8.3.3 Interference Estimation

An estimate of the inter-cell interference is found from

$$I_l = \frac{1}{9} \sum_{i=1}^{10} \left| h_{l,i}^{samp} - h_l^{est} \right|^2, \quad l = 1, \cdots, L$$

To be precise, the expectation value of I_l also contains inter-symbol interference from the cell we are trying to demodulate. That is, the different paths carry own copy of the sent signal and since they are not time-aligned, they will interfere with each other.

2.8.3.4 Signal-to-Interference Ratio (SIR)

SIR is defined as:

$$SIR = \sum_{l=1}^{L} \frac{\left| h_l^{est} \right|^2}{I_l}$$

and is computed once per slot. It is a quality measure of the propagation channel. The higher the ratio the lesser the errors will be made when determining the sent data.

2.8.3.5 Combiner

The sent symbol S is recovered by multiplying the RAKE output with the conjugate of the channel estimates, that is,

$$\sum_{l=1}^{L} \frac{\left(h_l^{est}\right)^* . r_l}{I_l} = \left(\sum_{l=1}^{L} \frac{\left(h_l^{est}\right)^* . h_l}{I_l} \right) . S$$

A real positive value is obtained if h_l^{est} is well estimated. We divide by I_l to favor paths experiencing low interference. Figure 2.8 shows the operations of a simple RAKE receiver with combiner output.

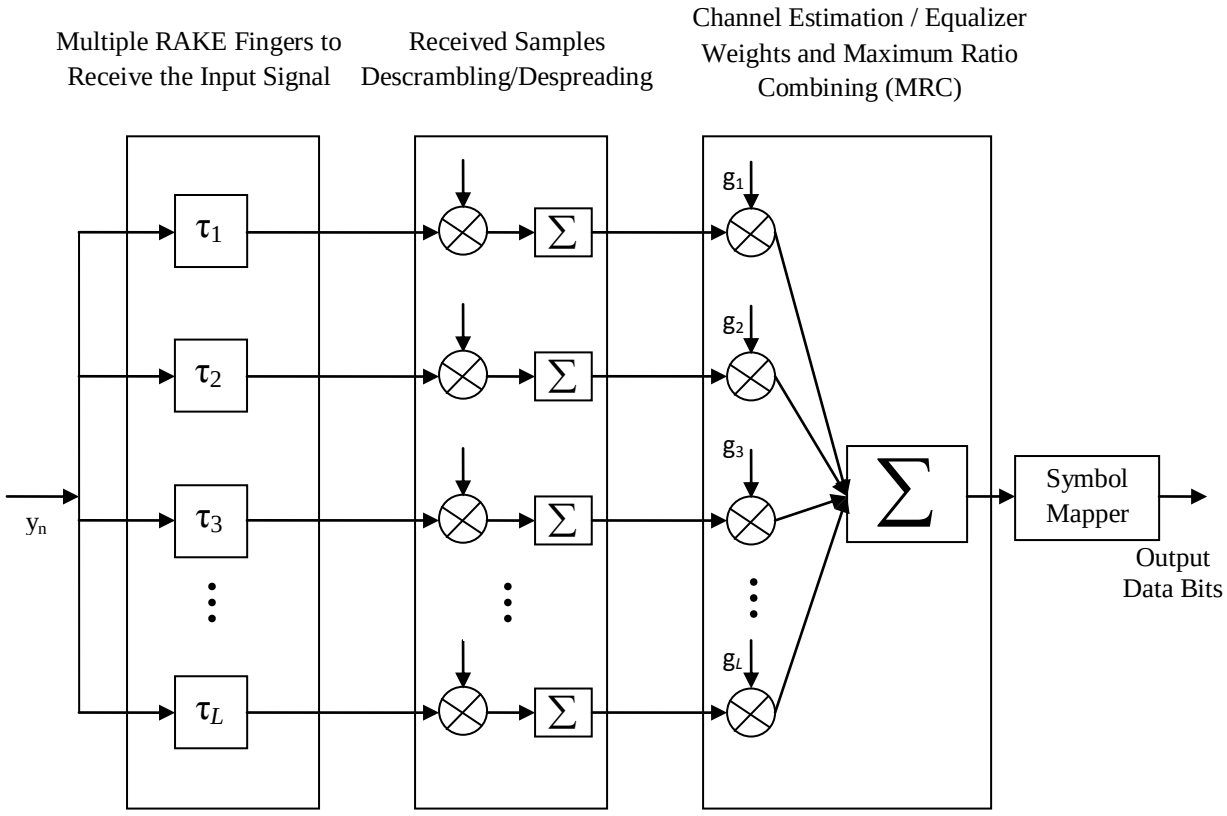

Figure 2.7: RAKE Receiver Block Diagram

Chapter 3

3 Equalizer Model

3.1 Communication System Diagram

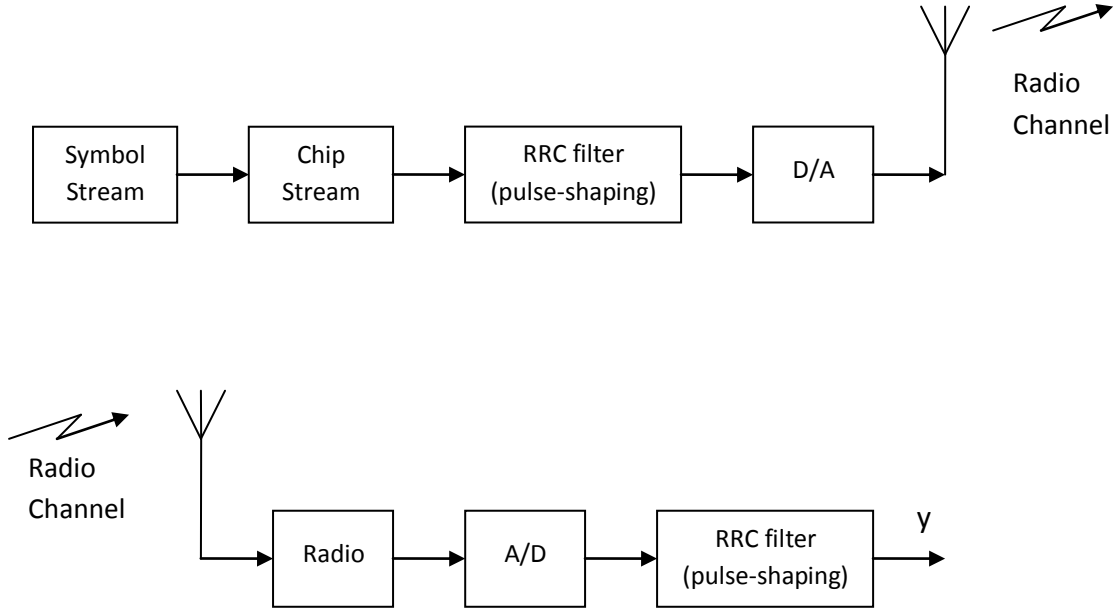

Figure 3.1: Communication System Block Diagram

3.2 RAKE (Time domain)

A simplified RAKE receiver block diagram is shown in figure 2.7. The filter (equalizer) weights shown in that figure can be determined in several ways for time domain equalization. Here, we consider the following two methods

1) Non-parametric MMSE-based Equalization
2) ML-based Equalization (Nonparametric GRAKE)

3.2.1 Non-parametric MMSE-based Equalization

Statistical signal model:

$$y_m = h_m s_0 + \underbrace{other\ chips/symbols\ transmitted\ \ from\ serving\ cell}_{(i)} + \underbrace{other\ \ chips/symbols\ transmitted\ \ from\ other\ \ cells}_{(ii)} + \underbrace{radio\ noise}_{(iii)} \tag{3.1}$$

where y_m is the received sampled signal (after descrambling/despreading), the sampling rate could be arbitrary (any os),

s_0 is the transmitted symbol/chip to demodulate, with $\|s_0\| = 1$,

h_m is the propagation channel including R_x & T_x radio filters affecting symbol/chip s_0 at time instant t_m, and

t_m is absolute sampling time.

Find a filter g that solves

$$\min_g E\left\{ \left| \sum_{m=-M}^{M} y_m g_m - s_0 \right|^2 \right\} \tag{3.2}$$

Here we assume that the time coefficients of g are placed on a fixed grid ranging from –*M* to *M*.

(P1): Also assume that s_0 is uncorrelated with the noise in term $(i), (ii)$ & (iii) in the statistical model.

Expanding (3.2) gives

$$\min_g \left[\vec{g}^H \underbrace{E\left\{ \vec{y}\,\vec{y}^H \right\}}_{=R_y^t} \vec{g} - \mathrm{Re}\, E\left\{ s_0^* \sum_{m=-M}^{M} y_m g_m \right\} \right] \tag{3.3}$$

where $\vec{g} = (g_{-M}, \cdots, g_0, \cdots, g_M)$,

$\vec{y} = (y_{-M}, \cdots, y_0, \cdots, y_M)$,

$\vec{y}^H = Hermitian\ \ Transpose\ \ of\ \ \vec{y}$, and

$\vec{g}^H = Hermitian\ \ Transpose\ \ of\ \ \vec{g}$

Since $\|s_0\|^2 = 1$, the assumptions in (P1) gives us

$$\mathrm{Re}\, E\left\{ s_0^* \sum_{m=-M}^{M} y_m g_m \right\} = \mathrm{Re} \sum_{m=-M}^{M} h_m g_m \qquad \left(\because s_0 s_0^* = \|s_0\|^2 = 1\right)$$

Thus (3.3) can be written as,

$$\min_g \left[\vec{g}^H \underbrace{E\left\{ \vec{y}\, \vec{y}^H \right\}}_{=R_y^t} \vec{g} - \mathrm{Re} \sum_{m=-M}^{M} h_m g_m \right] \tag{3.4}$$

Taking the derivate of (3.4) w.r.t g and solving for zero gives, see Appendix B

$$g = \left(R_y^t\right)^{-1} \vec{h}^* \tag{3.5}$$

where $\vec{h} = \left(h_{-M}, \cdots, h_0, \cdots, h_M\right)$ and by omitting the scalar multiplier in the (3.5).

Here R_y can be computed by filtering the received samples as

$$R_y(l,k) = \lambda \cdot R_y^{old}(l,k) + (1-\lambda) y_n^* y_{n-(k-l)} \tag{3.6}$$

where the filtering parameter λ depends on the Doppler spread.

3.2.2 ML-based Equalization (Non-parametric G-RAKE)

Referring back to (3.1)

$$y_m = h_m s_0 + n_m$$

where n_m is modeling the unwanted part of the received signal, that is, the noise.

Assume we have $m = 1, \cdots, M$ sampled y_m; collect them into a vector $\vec{y} = \left(y_1, \cdots, y_M\right)$. Let's then try to fit the vector $\vec{y}$ to a multi-dimensional probability distribution. A first choice is the Gaussian probability distribution, since it is simple to manipulate and contains few parameters to estimate.

Assuming the probability distribution for $\vec{y}$ to be Gaussian, we have the following *pdf*

$$e^{-\left(\vec{y}-\vec{h}s_0\right)^H R_n^{-1} \left(\vec{y}-\vec{h}s_0\right)} \tag{3.7}$$

where $\vec{h} = \left(h_{-M}, \cdots, h_0, \cdots, h_M\right)$

and R_n is the covariance matrix of the noise defined as

$$(R_n)_{m_1 m_2} = E\{ n_{m_1} n_{m_2}^* \}$$

Maximizing (3.7) with respect to s_0, that is, take the derivative of (3.7) with respect to s_0 and solve the result for s_0. Then, s_0 is given by

$$s_0 = \left(R_n^{t\,-1} \vec{h}^* \right)^t \vec{y}, \tag{3.8}$$

by omitting a scalar factor $\left(\vec{h}^H R_n^{-1} \vec{h} \right)^{-1}$.

Comparing with (3.5) shows that the filter g here is given by $\left(R_n^t \right)^{-1} \vec{h}^*$ and in (3.5) is given by $\left(R_y^t \right)^{-1} \vec{h}^*$.

Assuming the noise n_m is uncorrelated with $h_m s_0$, we have

$$\begin{aligned} R_y &= E\left\{ \left(\vec{h} s_0 + \vec{n} \right) \left(\vec{h} s_0 + \vec{n} \right)^H \right\} \\ &= \underbrace{|s_0|^2}_{=1} \vec{h} \vec{h}^H + E\{ \vec{n}\, \vec{n}^H \} = \vec{h} \vec{h}^H + R_n \end{aligned} \tag{3.9}$$

In practice, it is difficult to estimate R_n without knowing the sent symbol s_0. If, however, we have a pilot channel, modeled as

$$y_m = h_m p_0 + \tilde{n}_m \tag{3.10}$$

The noise $\tilde{n}_m$ is of the same nature as n_m (which is most often the case); we can now estimate R_n based on the pilot channel, that is,

$$(R_n)_{m_1 m_2} = \left(y_{m_1} p_0^* - h_{m_1}^{est} \right) \left(y_{m_2} p_0^* - h_{m_2}^{est} \right)^*$$

Here h_m^{est} is an averaged or filtered version of the samples $y_m p_0^*$, for example,

$$h_m^{est} = \lambda_h \left(y_m p_0^* \right) + (1 - \lambda_h) h_{m,old}^{est} \tag{3.11}$$

Also less variations in R_n can be had by applying filtering as below

$$R_n^{filt} = \lambda_{R_n} (R_n) + (1 - \lambda_{R_n}) R_{n,old}^{filt} \tag{3.12}$$

3.2.3 SIR

For both MMSE and ML methods, the demodulated symbol/chip is given by the following equation

$$s_0 = \left(R^{-1}\vec{h}^*\right)^t \vec{y}$$

where the matrix R is given by R_y^t if the filter g is computed using the MMSE method and R_n^t if the ML method is used.

Given the model in (3.1)

$$\vec{y} = \vec{h}s_0 + \vec{n} \qquad |s_0| = 1$$

by multiplying the above equation with the filter g, we get

$$\left(R^{-1}\vec{h}^*\right)^t \vec{y} = \left(R^{-1}\vec{h}^*\right)^t \vec{h}\, s_0 + \left(R^{-1}\vec{h}^*\right)^t \vec{n} \tag{3.13}$$

The signal-to-interfernce ratio is defined as

$$SIR = \frac{\left|\left(R^{-1}\vec{h}^*\right)^t \vec{h}\, s_0\right|^2}{E\left\{\left|\left(R^{-1}\vec{h}^*\right)^t \vec{n}\right|^2\right\}} = \frac{\left|\left(R^{-1}\vec{h}^*\right)^t \vec{h}\right|^2}{E\left\{\left(R^{-1}\vec{h}^*\right)^t \vec{n}\,\vec{n}^{*t}\left(R^{-1}\vec{h}^*\right)^*\right\}}$$

$$= \frac{\left|\left(R^{-1}\vec{h}^*\right)^t \vec{h}\right|^2}{\left(R^{-1}\vec{h}^*\right)^t E\left\{\vec{n}\,\vec{n}^{*t}\right\}\left(R^{-1}\vec{h}^*\right)^*} = \frac{\left|\left(R^{-1}\vec{h}^*\right)^t \vec{h}\right|^2}{\vec{h}^{*t}R^{-t}R_n\left(R^{-1}\vec{h}^*\right)^*}$$

For the ML method $R^{-t}R_n = I\left(identity\ matrix\right)$

$$\Rightarrow \qquad SIR = \frac{\left|\left(R^{-1}\vec{h}^*\right)^t \vec{h}\right|^2}{\left(\vec{h}^*\right)^t\left(R^{-1}\vec{h}^*\right)^*} = \frac{\left|\left(R^{-1}\vec{h}^*\right)^t \vec{h}\right|^2}{\left(\left(R^{-1}\vec{h}^*\right)^t \vec{h}\right)^*} = \left(R^{-1}\vec{h}^*\right)^t \vec{h}$$

For the MMSE method no such reduction is possible.

In practice, the numerator in SIR is replaced by $\left|\left(R^{-1}\vec{h}^*\right)^t \vec{y}\right|^2$. The expectation value of this is

$$\left|\left(R^{-1}\vec{h}^*\right)^t \vec{h}\right|^2 + E\left\{\left|\left(R^{-1}\vec{h}^*\right)^t \vec{n}\right|^2\right\}$$

$$\Rightarrow \qquad SIR_{practical} = SIR + 1$$

Also $E\left\{ \left| \left(R^{-1}\vec{h}^{*}\right)^{t}\vec{n} \right|^{2} \right\}$ in the denominator of SIR is computed by averaging the square of

$$\left(R^{-1}\vec{h}^{*}\right)^{t}\vec{y} - \left(R^{-1}\vec{h}^{*}\right)^{t}\vec{h}p = n_{sample} \tag{3.14}$$

Where p are known pilot symbols. From (3.13) we get that the above difference equals $\left(R^{-1}\vec{h}^{*}\right)^{t}\vec{n}$. Let $n_{sample,i}$ be a number of collected samples, then an estimate of $E\left\{ \left| \left(R^{-1}\vec{h}^{*}\right)^{t}\vec{n} \right|^{2} \right\}$ is given by

$$\frac{1}{\#Samples}\sum_{i=1}^{\#Samples}\left|n_{samples,i}\right|^{2}$$

If the ML-method is used and we are confident that the used R approximates well R_n^t, then the simplified expression $\left(R^{-1}\vec{h}^{*}\right)^{t}\vec{h}$ can be used for SIR.

3.3 FFT (Frequency domain)

3.3.1 System Model

Time domain signal $y(t)$ at the receiver is modeled as below

$$y(t) = \sum_{p=1}^{P}\sum_{m=-\infty}^{\infty}\sum_{l=1}^{L} h_l^{prop} a_p c_m^{(p)} \rho\left(t - m\Delta_{chip} - \tau_l\right) + noise, \tag{3.15}$$

where p enumerates the physical channels;
m enumerates the chips;
l enumerates the propagation paths;
h_l^{prop} is a complex valued propagation channel;
a_p is the signal amplitude;
$c_m^{(p)}$ is the chip at index m for p^{th} channel (composed of channelization code, scrambling code, and the sent symbol);
ρ is the pulse shaping filter; and
τ_l is the propagation path delay for signal path l.

Figure 3.2 shows the different blocks used in the FFT equalizer receiver. Functioning detail about respective blocks is provided in the coming sections.

3.3.2 Demodulation

Sample the received signal at $t_n = n\Delta_{chip}$, then

$$y_n = \sum_{p=1}^{P} \sum_{m=-\infty}^{\infty} a_p h_m^{(net)} c_{n-m}^{(p)} + noise = \sum_{p=1}^{P} \vec{h}^{(net)} * \; a_p \vec{c}^{(p)} + noise \tag{3.16}$$

where $*$ represents convolution,

$h_m^{(net)} = h(t_n)_l^{prop} \cdot \rho\left(t_n - m\Delta_{chip} - \tau_l\right)$, where t_n is the absolute time.

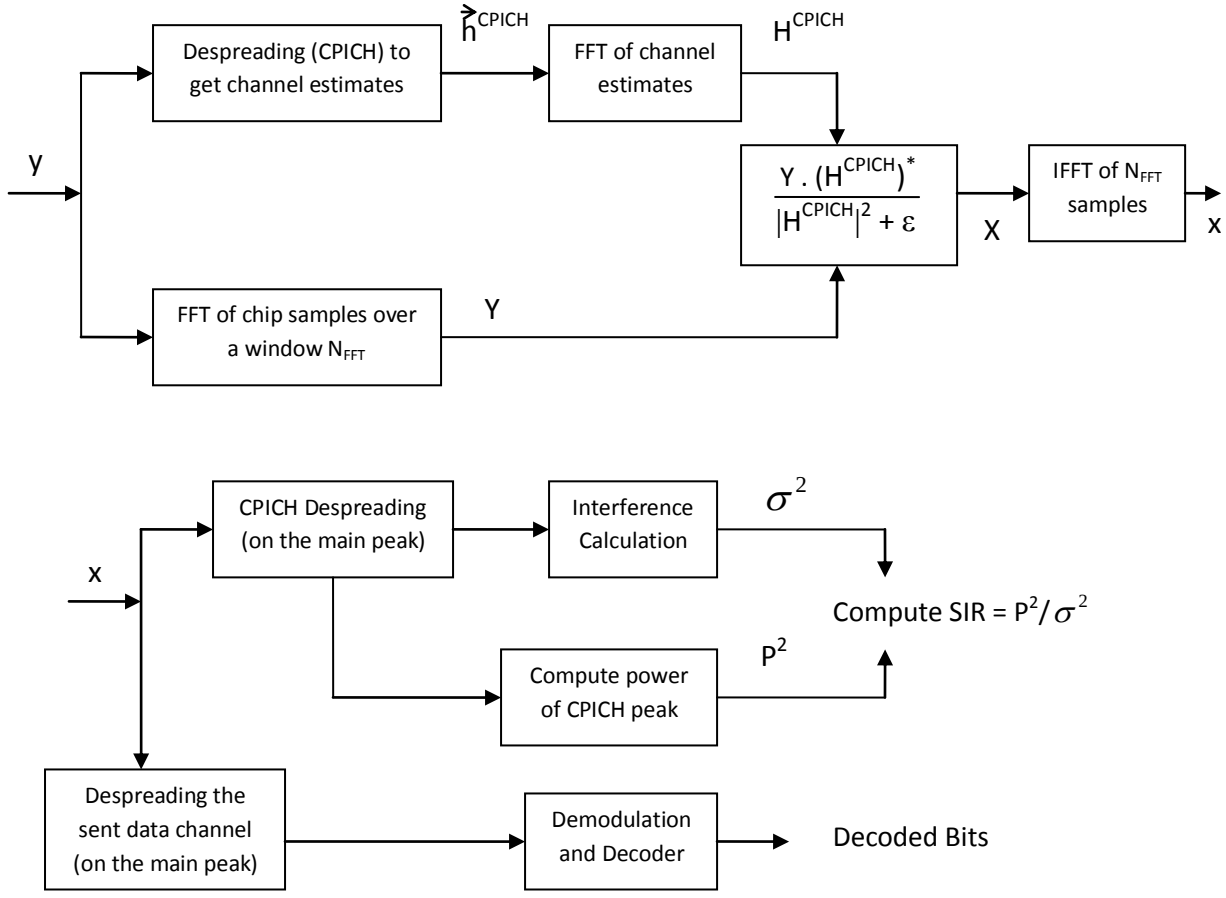

Figure 3.2: FFT Equalizer Receiver Block Diagram

Fourier transform of y_n will provide Y_n which can be described as follows

$$Y_n = \sum_{p=1}^{P} H_n^{(net)} \cdot C_n^{(p)} + noise \tag{3.17}$$

where $H_n^{(net)}$ is the Fourier transform of $\vec{h}^{(net)}$ and

$C_n^{(p)}$ is the Fourier transform of $a_p \vec{c}^{(p)}$

For the MMSE based equalizer, the influence of $H^{(net)}$ is removed to obtain X_n as shown below in equation (3.18)

$$X_n = Y_n \cdot \frac{\left(H_n^{(net)}\right)^*}{\left|H_n^{(net)}\right|^2 + \sigma^2} \tag{3.18}$$

where σ^2 is the estimate of noise variance and $\left(H_n^{(net)}\right)^*$ is the complex conjugate of $H_n^{(net)}$.

Eq. (3.18) refers to the MMSE based equalizer, which is explained next. Now referring back to (3.1): for a signal model

$$y = h \cdot s + noise$$

where *'s'* is the transmit symbol/chip. Find a filter *'w'*, such that the following expression is minimized:

$$\begin{aligned}
&\min_w E\left\{\left|y \cdot w - s\right|^2\right\} \\
&= \min_w E\left\{\left|h \cdot s \cdot w - s + w \cdot noise\right|^2\right\} \\
&= \min_w \left(\left|h \cdot s\right|^2 \cdot \left|w\right|^2 + \left|s\right|^2 + \left|w\right|^2 \cdot \sigma^2 - h \cdot s \cdot w \cdot s^* - \left(h \cdot s \cdot w\right)^* \cdot s\right) \\
&= \min_w \left(\left(\left|h \cdot s\right|^2 + \sigma^2\right) \cdot \left|w\right|^2 - 2\,\mathrm{Re}\left(h \cdot w\right)\right)
\end{aligned}$$

By solving for 'w' gives

$$w = \frac{h^*}{\left|h\right|^2 + \sigma^2}$$

$$\rightarrow \; s \; = \; y \cdot w \; = \; y \cdot \frac{h^*}{\left|h\right|^2 + \sigma^2}$$

In the simulations, we will use (3.19) for the required channel cancellation operation as follows:

$$X_n = Y_n \cdot \frac{\left(H_n^{(net)}\right)^*}{\left|H_n^{(net)}\right|^2 + \varepsilon} \tag{3.19}$$

where *'ε'* can be called a regularization term which needs to be tuned depending on the propagation channel profile and on the signal-to-noise ratio value at the receiver.

3.3.3 Approximations to investigate

The following approximations will be investigated:

1- The Fourier transform needs to be finite, that is, a finite number of samples can only be handled at a time. Investigate optimal (smallest) number of samples for different channels.
2- The amount of filtering needs to be tuned for filtered channel estimate $h_{filtered,n}^{(net)}$ as shown in (3.23).
3- The amount of filtering needs to be tuned for interference estimation $\sigma_{filtered,k}^2$ as shown in (3.22).

3.3.4 Interference Calculation

After applying IFFT on X_n to come back to time domain, we get '*x*' which can be modeled as

$$x_n = \sum_{p=1}^{P} a_p c_n^{(p)} + noise \tag{3.19}$$

Assume $p=1$ for the CPICH. Despreading of *'x'* with the scrambling code and then the channelization code of $p=1$ will give

$$\frac{1}{256} \sum_{n=1+(k-1)256}^{256k} x_n . \left(c_n^{(1)}\right)^* = x_{sample,k}^{CPICH} \tag{3.20}$$

where *'k'* refers to the CPICH symbols received by despreading of the chip samples. Ten CPICH symbols are received from one WCDMA slot.

The received CPICH symbols are filtered as below:

$$x_{filtered,k}^{CPICH} = (1-\lambda_h).x_{filtered,k-1}^{CPICH} + \lambda_h\, x_{sample,k}^{CPICH}$$

The interference is further estimated as,

$$\left|x_{filtered,k}^{CPICH} - x_{sample,k}^{CPICH}\right|^2 = \sigma_{sample,k}^2 \ , \tag{3.21}$$

To get the final σ^2, filter $\sigma^2_{sample,k}$

$\sigma^2 = \sigma^2_{filtered,k}$, where

$$\sigma^2_{filtered,k} = (1-\lambda_\sigma)\sigma^2_{filtered,k-1} + \lambda_\sigma \sigma^2_{sample,k} \quad (3.22)$$

3.3.5 Power Calculation

To calculate the received signal power, let $p_{est} = \left| x^{CPICH}_{filtered,k} \right|^2$. Filter p_{est} as in (3.22) and call it P.

3.3.6 Calculation of Filtered Channel Estimate

Put RAKE fingers on all N_{FFT} samples used in the FFT of y_n, despread these fingers using the CPICH channelization code. If the CPICH is for $p=1$, then

$$h^{(net)}_{sample,r} = \frac{1}{256}\sum_{n=1}^{256} y_{n+r-1} \cdot \left(c^{(1)}_n\right)^*, \qquad r = 1, \cdots, N_{FFT}$$

where *'r'* is the RAKE finger index and $\left(c^{(1)}_n\right)^*$ includes the complex conjugate of scrambling code, channelization code for the CPICH, and sent QPSK pilot symbol.

Assume $\vec{h}^{(net)}_{sample,n} = \left(h^{(net)}_1, h^{(net)}_2, \cdots, h^{(net)}_{N_{FFT}}\right)$, and then filter $\vec{h}^{(net)}_{sample,n}$ as shown in (3.23) to get $\vec{h}^{(net)}_{filtered,n}$.

$$\vec{h}^{(net)}_{filtered,n} = (1-\lambda_h)\vec{h}^{(net)}_{filtered,n-1} + \lambda_h \vec{h}^{(net)}_{sample,n} \quad (3.23)$$

$\vec{h}^{(net)}_{filtered,n}$ is also alternatively called as $\vec{h}^{CPICH}_{filtered,n}$ in this thesis.

Chapter 4

4 Implementation and Results

4.1 Simulation Setup

Both the methods described in sections 3.2 and 3.3 for channel equalization are implemented in IT++. Standard library features of IT++ are used to construct different blocks of the transmitter, receiver, and the propagation channel. Simulation parameters used for the WCDMA transmit signal are given below.

With reference to figure 2.1, OVSF code tree, the channelization codes used in the simulations are shown in table 4.1.

Table 4.1: Simulation setup: different users/channels with their *sf* and power assigned

USER	Channelization Code	Spreading Factor	Power (EcIor)
CPICH	$C_{(256,1)}$	256	-10 dB
Data (desired user)	$C_{(16,2)}$	16	-11 dB
user1	$C_{(128,4)}$	128	0 dB [(1)]
user2	$C_{(128,5)}$	128	-2 dB [(1)]
user3	$C_{(128,6)}$	128	-4 dB [(1)]
user4	$C_{(128,7)}$	128	-1 dB [(1)]

Powers assigned to the other users, from user1 to user4 as shown in Table 4.1 are relative power values to each other, i.e., after assigning power to CPICH and data, power values for other users are calculated based on these relative power values such that the total power remains one.

[(1)] The spreading factor and assigned power of the other four users (user1 to user4) are based on the reference table *"Table C.13A: OCNS definition for HSDPA receiver testing"*, 3GPP TS 25.101 V8.4.0 (2008-09).

4.1.1 Transmit Signal from Node B

Figure 4.2 shows the simulation flow to construct a WCDMA transmit signal at Node B which carries information for all the users/channels mentioned in table 4.1. The information for different users/channels is spread with the use of their respective channelization codes. Scrambling code used at the BS (Node B) is marked as 'sc1' which is uniquely assigned to the BS. And any other scrambling code may be employed for transmission from other BS.

CPICH uses all zero bits, whereas, random bits are generated for other users as well as for the desired data user. QPSK is used as the modulation scheme for both for the data users and for CPICH.

Half slot processing is employed, i.e., 1280 chips are processed at one time. Same channelization codes are used each time to spread the different data symbols, while scrambling code is repeated after every 38400 chips. Spreading factor of 16 for the data user implies that 1280/16 = 80 QPSK data symbols can be transmitted through each half slot. Similarly, 5 CPICH symbols and 10 other data user's symbols are transmitted at one time.

Before scrambling, each user/channel signal is multiplied with its respective amplitude. The signal amplitudes are calculated based on the signal power values mentioned in table 4.1 and the overall signal energy is kept as unity.

Root raised cosine (RRC) filter with roll-off factor = 0.22, over sampling rate = 4, and filter length = 14 chips is used. Up-sampling by a factor 4 is done which provides 5120 signal values after the transmit filter.

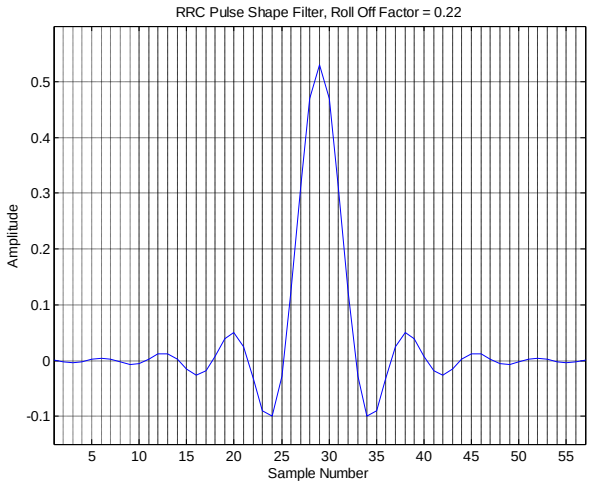

Figure 4.1: Root Raised Cosine Filter; sample rate = 4 per chip, filter length = 14chips

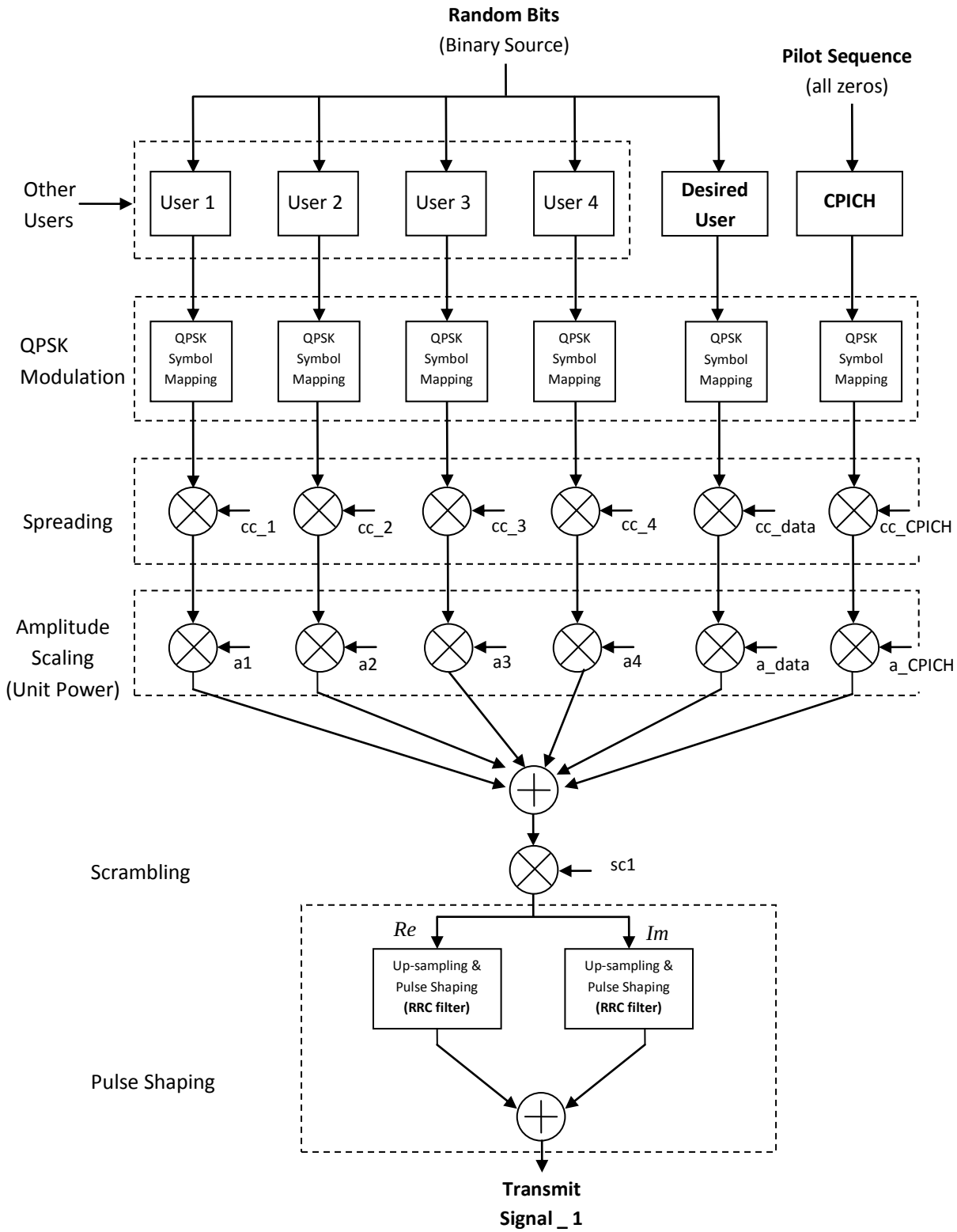

Figure 4.2: Transmission of WCDMA signal from Node B

4.1.2 Propagation Channel

The propagation channel model used in the simulations is a two path non-fading (static) channel. The power is divided equally between the two paths. Different values of delay spread are simulated; and the results are shown in section 4.4 and onwards. Single path channel model and ITU-Pedestrian B with speed 3km/hr (PB3) which is a slow fading channel; are also used in the simulations.

4.1.3 Signal Reception at UE

The up-sampled signal values are received at UE through a propagation channel. The receiver functions are shown in figure 4.3. WCDMA signal from the desired BS as well as from another nearby BS, which is using a different scrambling code, is received at MS through a wireless channel.

Additive White Gaussian Noise (AWGN) is added to the received signal. Equalizer performances on different values of noise variance are tested by various simulations. Also without AWGN, equalizer performance is observed. Frequency errors are generated at the UE due to any phase offset or synchronization loss between the clocks of the BS and MS. Receiver performance with and without frequency errors are then tested. Analog-to-Digital converter (A/D) is used to digitize the received signal before filtering operation. Equalizers performance with different (A/D) converters are simulated and shown in the results section 4.4.

Received signal is finally fed to the receiver filter which is also a root raised cosine (RRC) filter matched to the transmit filter. Matched filter output is then used for both equalizers.

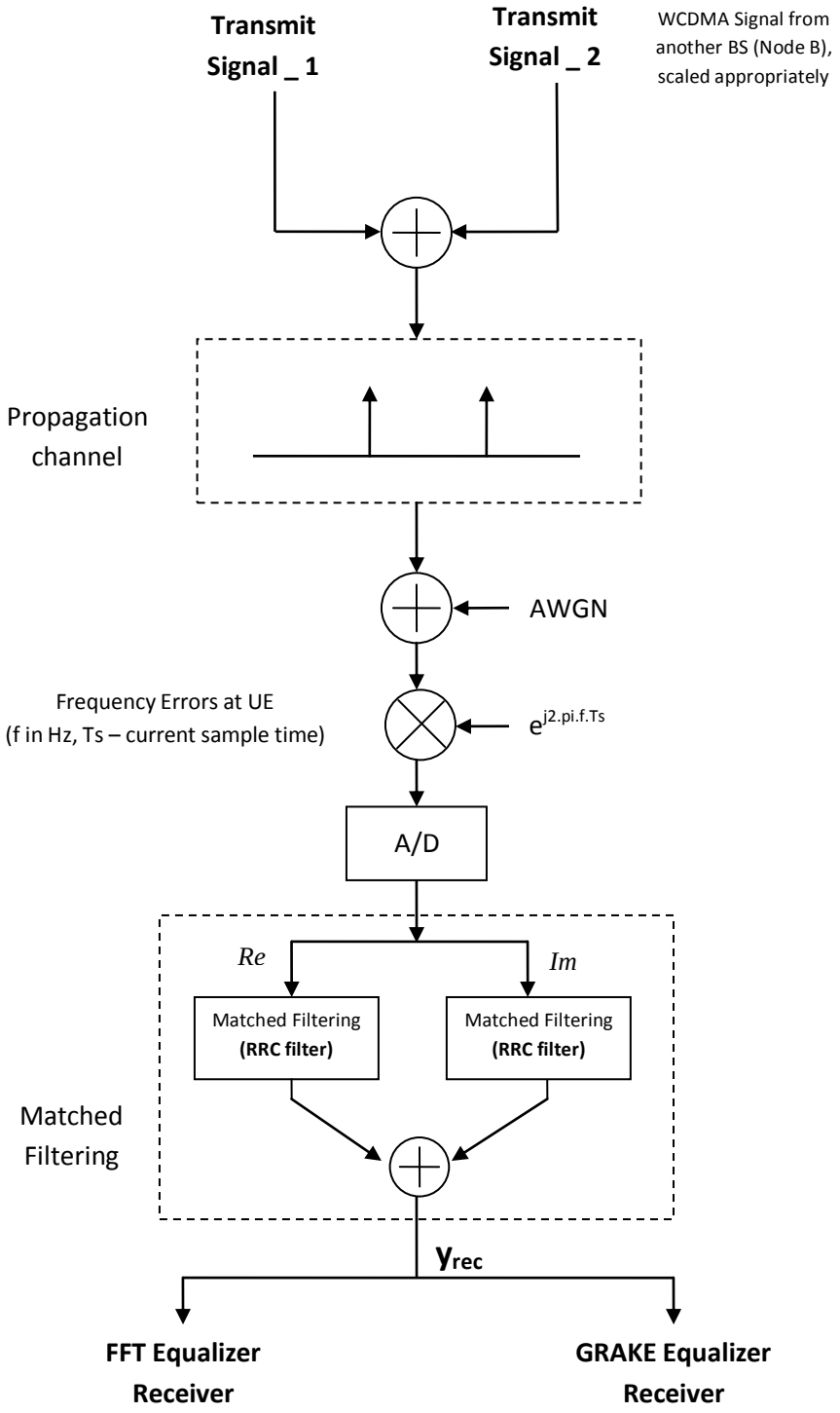

Figure 4.3: Received Signal at UE via Matched Filtering

4.2 GRAKE Equalizer Receiver

4.2.1 Channel Estimation

Received signal values after the receiver filter are used to detect the channel response to the transmit signal. In figure 4.4**,** different blocks are shown which are used in the simulator to detect the channel response on different signals received via multiple rake fingers.

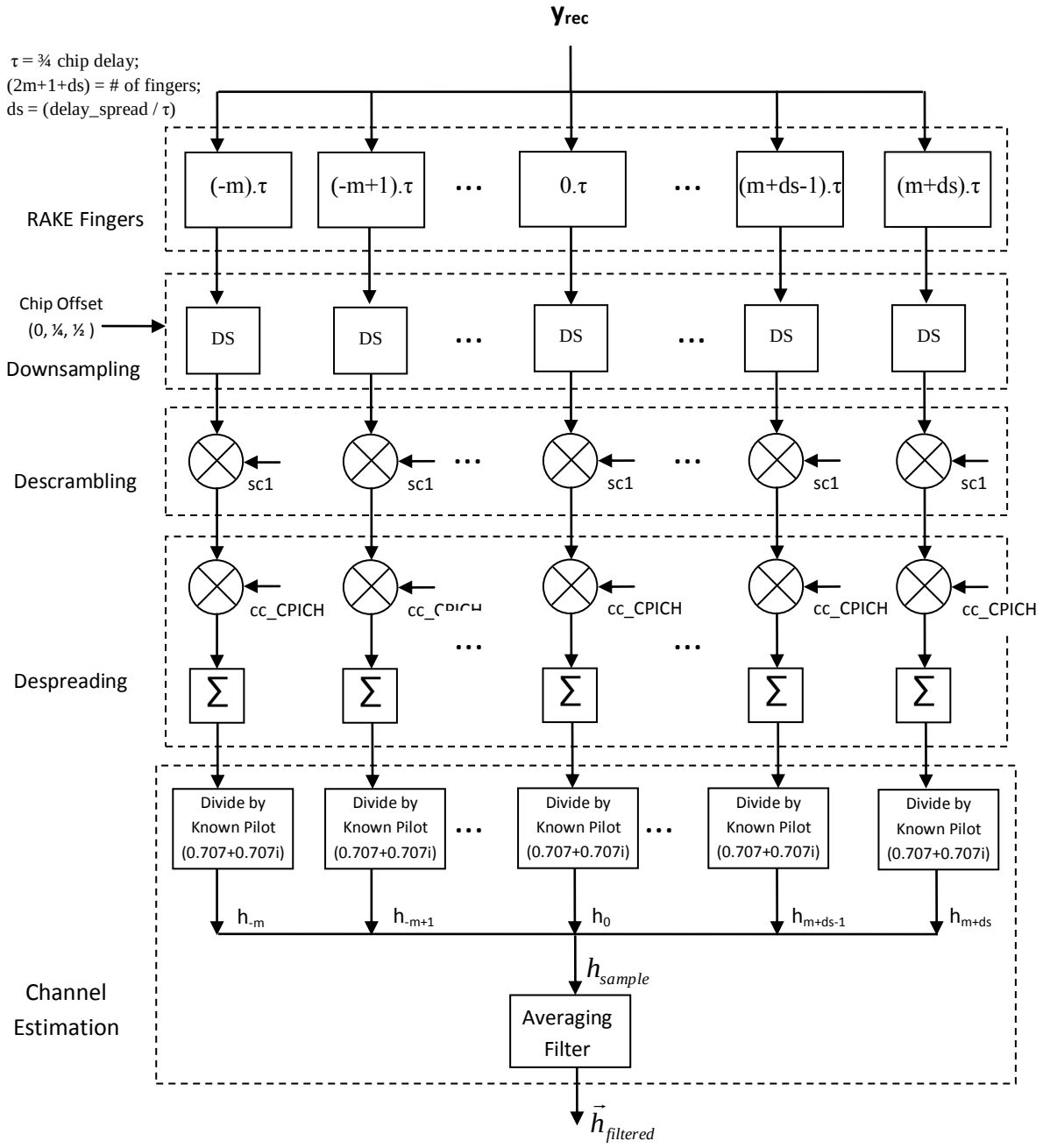

Figure 4.4: Non-Parametric G-RAKE Receiver Channel Estimation

GRAKE uses (2m+1+ds) fingers which are separated by a fixed time delay between any two rake fingers, i.e., 'τ' equals to ¾ chip delay. Different delayed versions of the WCDMA signal are received via these fingers. Depending on the R_x & T_x filter length, the parameter 'm' is selected as 20 = 15/τ, to collect all the energy stored in the filter taps; while 'ds' is the delay spread (time difference between LOS signal path and the last significant signal energy path) divided by the finger spacing (τ). In this thesis 'ds' or path delay will be referring to the delay (in # of chips) between two equal energy signal paths. RAKE finger placed at (0.τ) implies zero delay is introduced and direct despreading is used. For single path test cases, nine fingers with fifth finger at the zero delay position are used in the test simulations (nine fingers are considered to be optimum number in this case).

Downsampling is performed on each rake finger as there is upsampling done at the transmitter side before transmission. Different offset positions are used as shown in the figure 4.3 to simulate the GRAKE equalizer performance for the time offset received data. Descrambling and despreading operations are implemented to recover the original sent symbols. Desired scrambling code 'sc1' for the BS scrambling and 'cc_CPICH' is used for the CPICH channel. Since the CPICH symbols are known at the UE, dividing with the known symbols return the channels estimate values on the respective rake fingers. Since five CPICH symbols are received in one half slot, averaging filter is implemented to filter the sampled channel estimates. The filtered channel estimate is then used for the estimation of noise covariance matrix and further the G-RAKE equalizer filter weights.

4.2.2 Equalizer Filter and SIR

Based on the sampled channel values and the filtered estimate, noise covariance matrix is calculated as shown in figure 4.5. Further, filtered channel estimate and filtered noise covariance matrix are used to determine the equalizer filter weights and an estimate of Signal-to-Interference ratio. Noise covariance matrix inversion is implemented by using standard built-in functions available in IT++ for calculating matrix inverse.

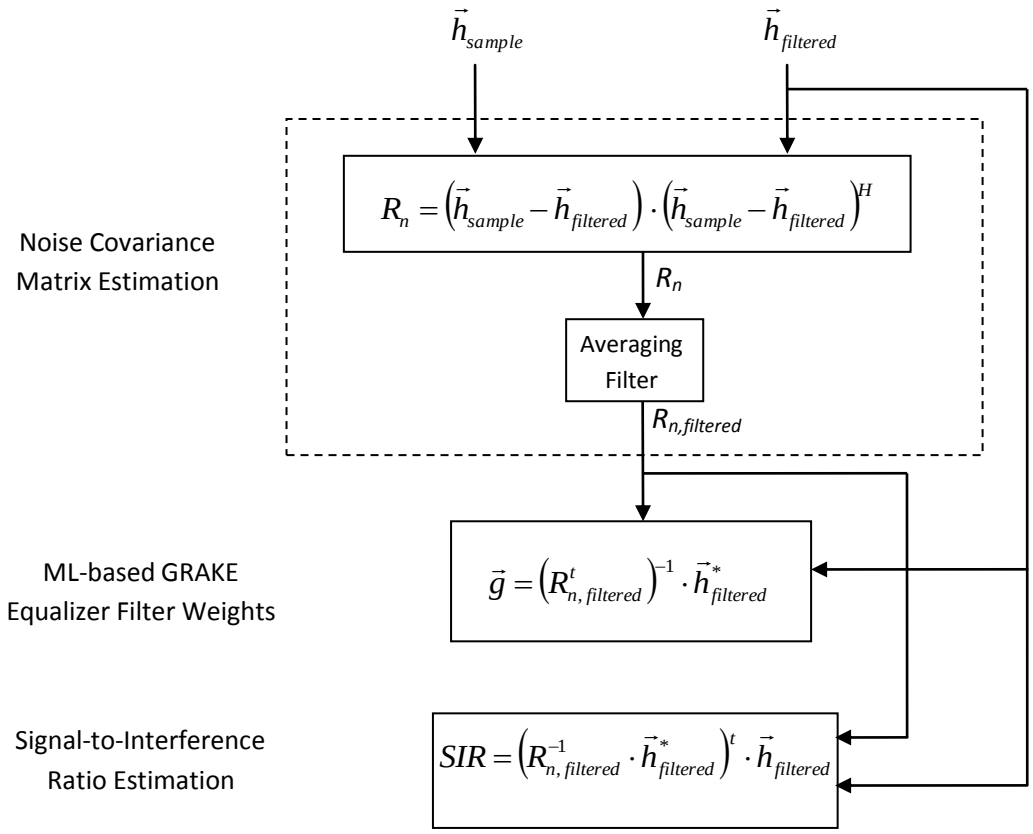

Figure 4.5: Non-Parametric G-RAKE Equalizer Filter and SIR

4.2.3 Combiner

Different delayed version of the received WCDMA signal are despread as is done in the GRAKE channel estimation, but now with the desired user channelization code, i.e., cc_data. Filter weights calculated above are now applied on the despread data symbols obtained from different rake fingers. Combiner operations are shown in figure 4.6.

Following the combiner output, QPSK demodulation is performed to recover the sent data bits. Received data bits are then compared with the original sent bits to calculate the bit error rate (BER).

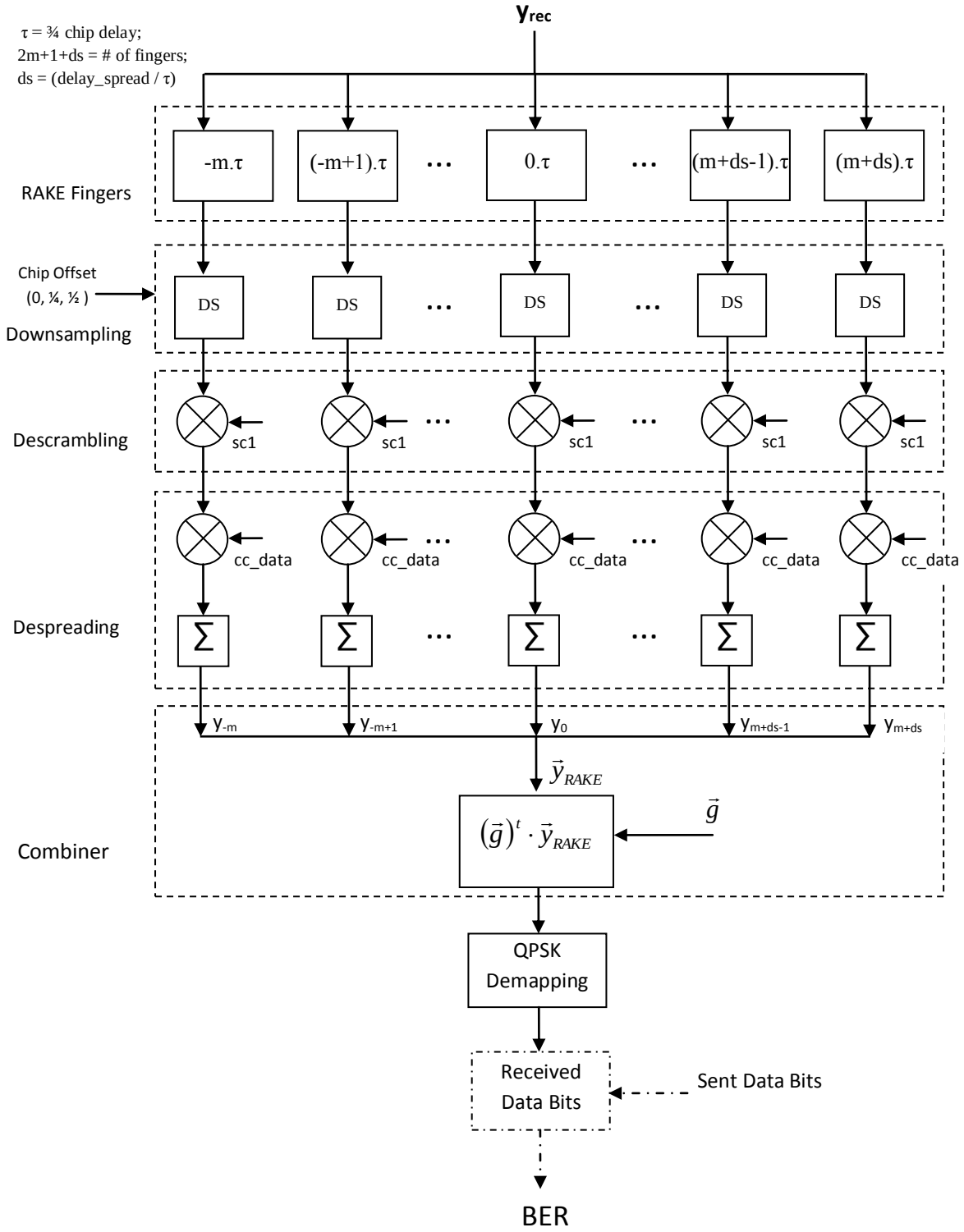

Figure 4.6: Non-Parametric G-RAKE Combiner Output and BER

4.3 FFT Equalizer Receiver

4.3.1 Channel Estimation

In the FFT receiver, the received signal is firstly down-sampled to over-sampling 1, that is, one sample per chip, see section 3.3.2. Multiple despreaders are then utilized to calculate the channel sample values as shown in figure 4.7. In FFT case, the despreaders are always

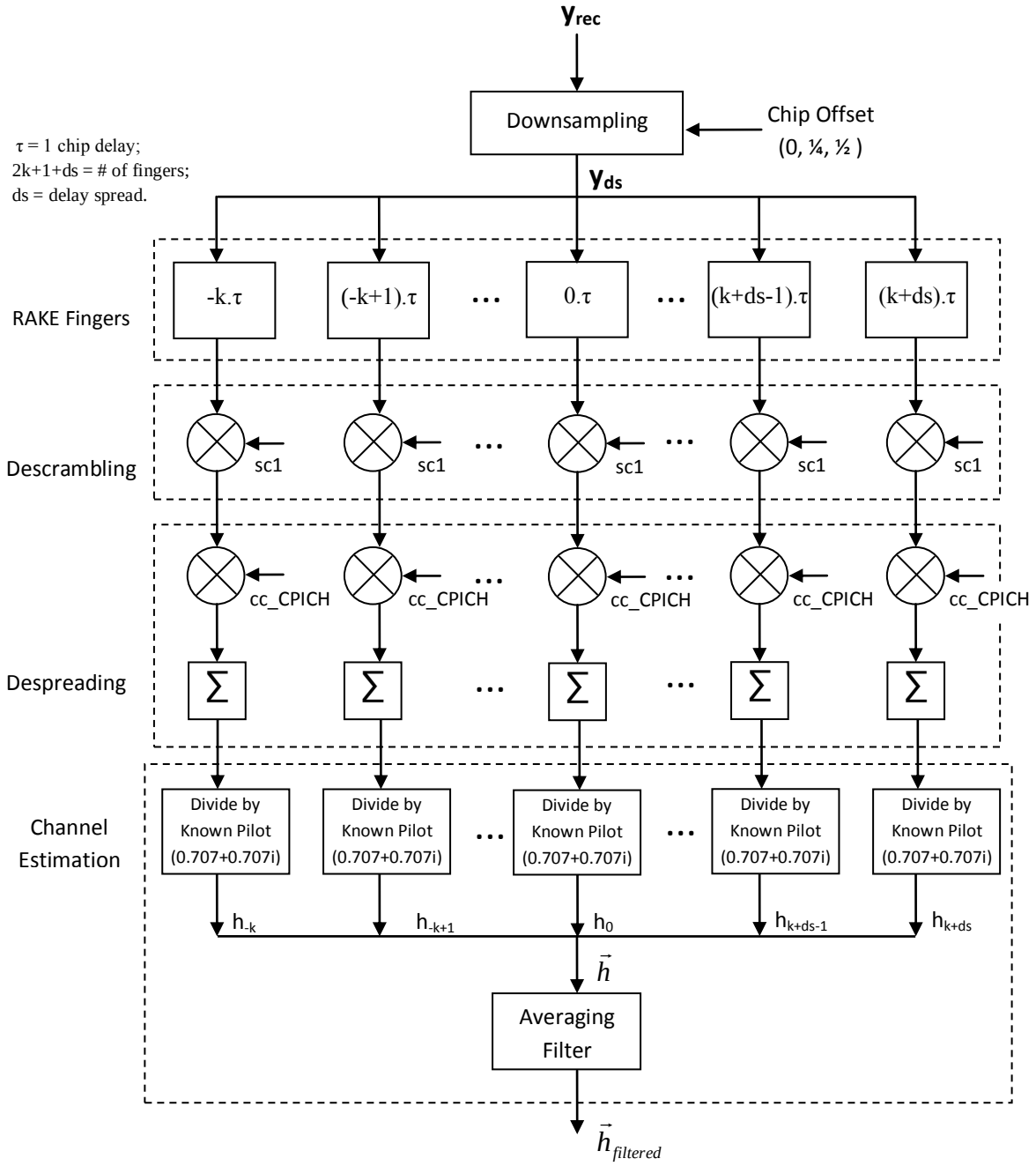

Figure 4.7: FFT Receiver Channel Estimation

separated by one chip delay while descrambling and despreading operations to get the channel sample values are the same as performed in the GRAKE channel estimation.

Based on the R_x & T_x radio filters which are used as standard root raised cosine filters with filter length equals to 14 chips as shown in figure 4.1, the parameter 'k', i.e., the number of despreaders used in the left of the main peak is chosen as 15; while the number of despreaders towards the right of the main peak are chosen as (15+ds). For single path test cases, ds = 0 is used. In that case, 31 despreaders are used to calculate the channel estimate, 15 despreaders on both sides of the zero delay despreader.

4.3.2 Equalizer

Equalization operation is performed in the frequency domain. Both the channel estimates values and received down sampled signal is converted to frequency domain by taking Fast Fourier Transform (FFT). FFT function is used as a standard IT++ library function. Figure 4.8 shows the method used in the FFT equalization operation.

The channel equalization is performed on each half slot received. The channel estimate vector used in the FFT equalizer has 1280 chips with the channel estimate values obtained by (2k+1+ds) despreaders in the centre and rest of the values as zeros.

A parameter tuning block as shown in figure 4.8 is also used in the FFT equalizer method for parameters tuning. An output of the intelligent block, 'ε' is required in the channel equalization operation. The value of 'ε' depends on the values of IorIoc, delay spread, and the size of the A/D used. Optimal values of 'ε' are found for different values of IorIoc and delay spread. The optimal values of 'ε' needs to be scaled with the same A/D constant (K) used for multiplying the signal before quantization. Different A/D sizes and their respective A/D constant (K) values are used in the simulations.

As the equalization is performed in the frequency domain, so an inverse Fourier Transform (IFFT) is used to convert the equalized signal back to the time domain signal. In the figure, it is also shown that the number of chips that can be used further for despreading and symbol detection is decided by the parameter tuning block's output 'M'. The value of M depends on the delay spread and target BER. For small delay spread channels, more chips are equalized as compared to large delay spread channels. More details about the number of output chip samples are given in section 4.4.6.1.

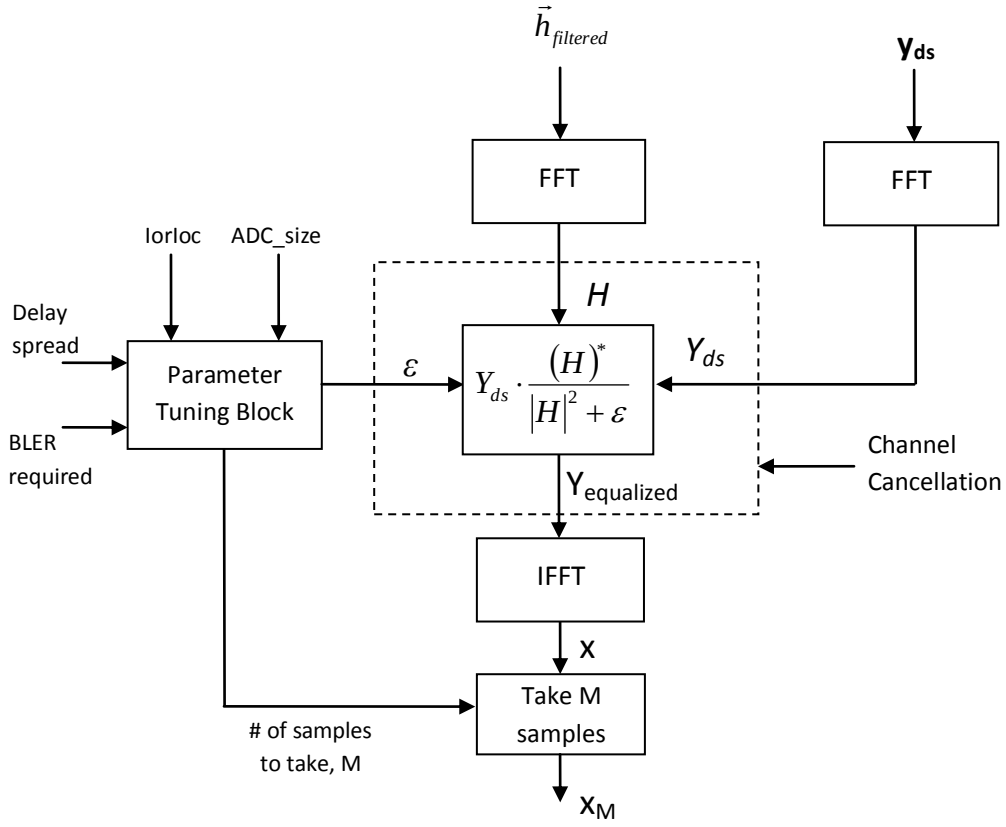

Figure 4.8: FFT Equalizer Input/Output Block Diagram

4.3.3 Despreader Output, BER, and SIR Estimate

Two despreaders are shown in figure 4.9, which are used to receive the CPICH symbols and desired data user symbols. Received data symbols are QPSK demodulated to recover the data bits and original sent bits are compared with the received bits to calculate the BER.

As there are five CPICH symbols received in one half slot, received CPICH symbols are filtered by using a first order recursive filter. The filtered CPICH symbol is used to calculate the signal power; while interference is estimated from the filtered CPICH symbol and sampled value of the CPICH symbol. Both these values are used to estimate the SIR.

Two other despreaders are also used in the simulations, though they are not shown in the figure. They are placed at one chip offset on both sides of the main peak CPICH despreader used for CPICH symbols. The estimated SIR of these three despreaders is then used to check if down sampling has been done at some time offset other than zero at the receiver or not.

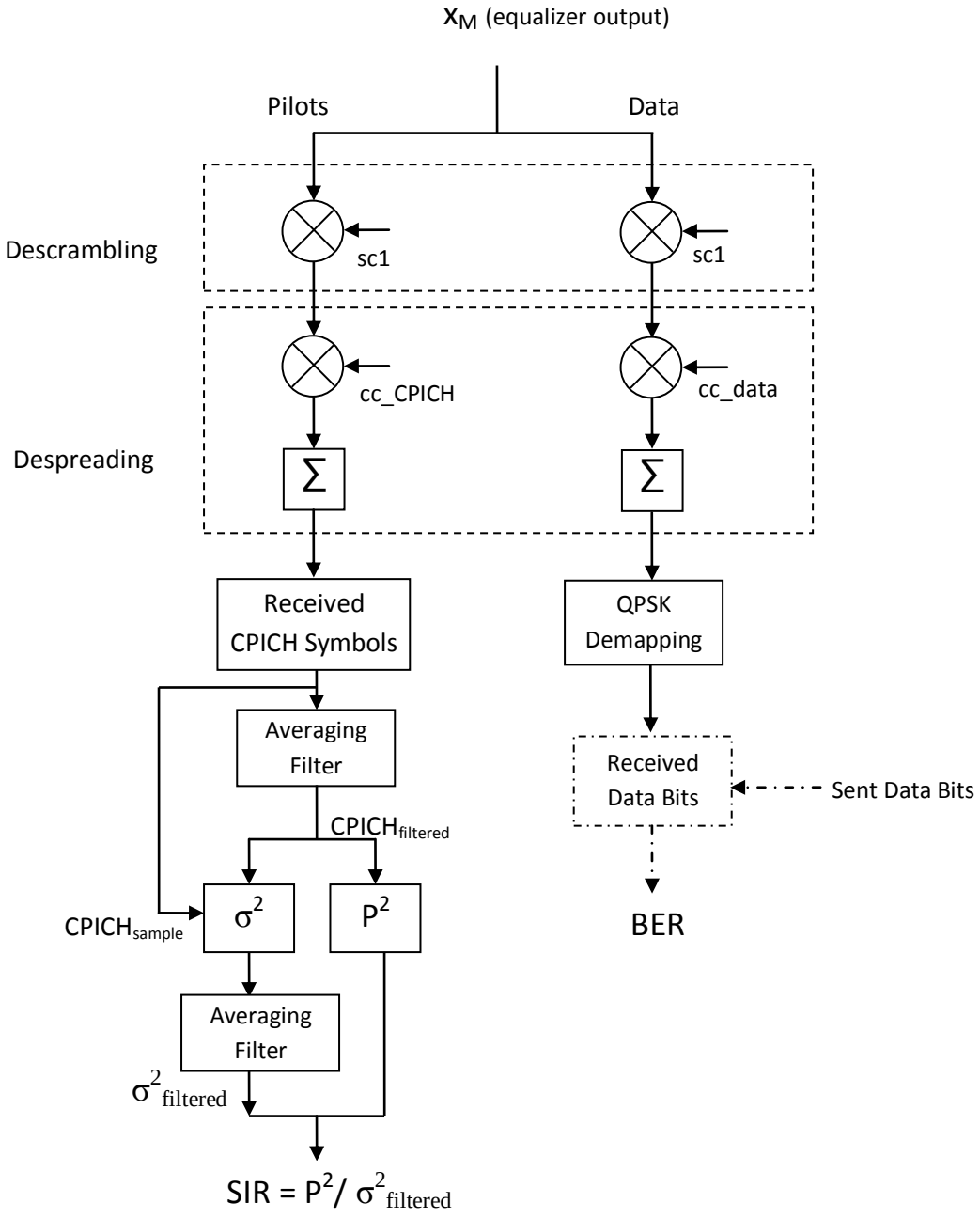

Figure 4.9: FFT Despreader Output, BER, and SIR Estimate

4.4 Results and Discussion

4.4.1 Parameters Optimization

4.4.1.1 GRAKE Parameters Optimization

Two averaging filters are implemented in the G-RAKE method. The averaging filter which is used to filter the channel estimate results uses λ_h; and the second filter which is filtering the noise covariance matrix uses λ_{R_n} as the filtering parameters as shown in (3.11) and (3.12) respectively.

Simulations are performed for different channels (single path and two path non-fading or static channels) and using different IorIoc values. For single path channel, nine fingers are used to receive the WCDMA signal. And for two path channel, number of fingers used to receive the WCDMA signal is calculated as (2m+1+ds), as discussed in section 4.2. Delay spread 'ds' = 5 chip is used for two path channel simulations.

Firstly, for an arbitrary value of λ_h equals to 1/200 for our case, multiple simulations are performed for IorIoc values starting from -4 dB and going up till 28 dB. For each IorIoc value, a range of values for λ_{R_n} from 1/25 to 1/500 are simulated. From the simulation results, BER performance of the data user is observed. Based on these results, optimum (largest) value for λ_{R_n} is selected to be 1/200, for all the IorIoc values as well as for the two main test cases, i.e., single path and two path channel with 'ds' = 5 chip. A large value of λ_{R_n} is used to give more weightage to the noise samples received in the current WCDMA slot.

Secondly, using the optimized value of λ_{R_n} = 1/200, another set of simulations are performed for a range of values of λ_h ranging from 1/25 to 1/500. Though, no significant influence on the BER performance is observed in these simulations for the different values of λ_h. One optimum value selected for λ_h is found as 1/100.

4.4.1.2 FFT Parameters Optimization

The FFT method for the frequency domain equalization is used by first converting the time domain signal to frequency domain and then the equalized signal is converted back to time

domain for despreading. To implement these operations, Fast Fourier Transform (FFT) and Inverse Fast Fourier Transform (IFFT) are used in the simulations. So, possible FFT window size is first determined which can be used for this equalization method.

Multiple simulations are performed with FFT window sizes: 32, 64, 128, 256, 512, 1024, and 2048. Two path static channel model with delay spread = 1, 5, 10, and 70 chips is used. From BER results of the desired data user, noise floor without AWGN is observed. Table 4.2 shows the BER results for a two path channel with delay spread = 5 chip, using different FFT window sizes and for different values of ε. **I**n these simulations, filtering parameter λ_h = 1/200 is used to filter the channel sample values to get a filtered channel estimate. Different simulation results are obtained using large delay spread values, such as, ds = 10 and 70 chip. The obtained results show that FFT window size = 2048 is to be selected, because, with bigger FFT window size larger delay spread can be equalized better as compared to smaller FFT window size.

Later, in all the FFT method simulations N_{FFT} = 2048 is opted to use for the FFT equalizer. FFT equalizer performance results with λ_h = 1/200, N_{FFT} = 2048, without AWGN, and for different delay spread values is shown in table 4.3. Without AWGN, optimum values of ε are selected for different delay spread values, e.g., ε is chosen as 1/2000 for 'ds' = 1 chip and 1/500 for all other delay spread values. ε = 0 is found to be optimum value for single path scenario as it gives BER = 0, if there is no AWGN.

By selecting appropriate values of ε mentioned above, then optimized values for the filtering parameter λ_h is determined for these different propagation channels. Now by using different IorIoc values from -4 dB to 28 dB, the BER performance results are obtained for the same set of delay spread values (1, 5, 10, and 70 chip) as well for the single path channel. It is found that λ_h = 1/200 is to be used for all the IorIoc values and for all the channels models (single path, two path with different delay spreads). Also, the filtering parameter λ_{CPICH}, used for the receive CPICH symbols filtering, is assigned the same value as is obtained for λ_h, i.e., λ_{CPICH} = 1/200 is used in the simulations estimating SIR values.

Table 4.2: N_{FFT} vs BER for two path channel, 'ds' = 5 chip, λ_h = 1/200, without AWGN

Sr. #	$1/\varepsilon$	BER vs N_{FFT} (FFT window size)					
		N_{FFT} = 64	N_{FFT} = 128	N_{FFT} = 256	N_{FFT} = 512	N_{FFT} = 1024	N_{FFT} = 2048
1	100	1.8E-03	1.8E-03	1.5E-03	1.5E-03	1.7E-03	1.6E-03
2	200	9.3E-04	4.0E-04	3.2E-04	3.2E-04	3.5E-04	4.1E-04
3	300	1.1E-03	1.6E-04	9.9E-05	9.9E-05	1.3E-04	1.6E-04
4	400	1.8E-03	6.3E-05	2.1E-05	2.1E-05	3.6E-05	7.5E-05
5	**500**	3.1E-03	3.6E-05	1.6E-05	1.6E-05	3.1E-05	4.2E-05
6	600	4.6E-03	3.1E-05	1.0E-05	1.0E-05	2.1E-05	1.9E-05
7	700	6.4E-03	3.1E-05	1.0E-05	1.0E-05	1.6E-05	1.4E-05
8	800	8.3E-03	4.2E-05	1.0E-05	1.0E-05	5.2E-06	7.8E-06
9	900	1.0E-02	4.2E-05	1.0E-05	1.0E-05	5.2E-06	3.1E-06
10	1000	1.3E-02	9.9E-05	1.0E-05	1.0E-05	0.0E+00	3.1E-06
11	1100	1.5E-02	1.7E-04	5.2E-06	5.2E-06	0.0E+00	1.6E-06
12	1200	1.7E-02	2.6E-04	5.2E-06	5.2E-06	0.0E+00	0.0E+00
13	1300	1.9E-02	3.5E-04	5.2E-06	5.2E-06	0.0E+00	0.0E+00
14	1400	2.1E-02	4.9E-04	5.2E-06	5.2E-06	0.0E+00	0.0E+00
15	1500	2.3E-02	5.9E-04	5.2E-06	5.2E-06	0.0E+00	0.0E+00
16	1600	2.5E-02	7.7E-04	5.2E-06	5.2E-06	0.0E+00	0.0E+00
17	1700	2.7E-02	9.8E-04	5.2E-06	5.2E-06	0.0E+00	0.0E+00
18	1800	2.9E-02	1.3E-03	5.2E-06	5.2E-06	0.0E+00	0.0E+00
19	1900	3.1E-02	1.5E-03	5.2E-06	5.2E-06	0.0E+00	0.0E+00
20	2000	3.3E-02	1.8E-03	5.2E-06	5.2E-06	0.0E+00	0.0E+00

One last optimization parameter for FFT method is λ_σ which is used to filter the interference estimate values. λ_σ is determined using the same set of IorIoc values (-4dB to 28dB) and using the same single path and two path channel models. For tuning λ_σ, variance of the SIR estimates of different WCDMA half slots (approx. 1200 half slots) is optimized. From the simulation results, i.e., variance of the SIR estimates, λ_σ = 1/100 is found as the optimized value.

Table 4.3: FFT Equalizer BER results for different delay spread values, N_{FFT} = 2048, without AWGN, λ_h = 1/200,

Sr. #	1 / ε	BER vs Delay Spread			
		1 chip	5 chip	10 chip	70 chip
1	100	0.603%	0.164%	0.105%	0.106%
2	200	0.312%	0.041%	0.017%	0.027%
3	300	0.200%	0.016%	0.006%	0.013%
4	400	0.141%	0.008%	0.002%	0.009%
5	500	0.101%	**0.004%**	**0.001%**	**0.007%**
6	600	0.076%	0.002%	0.001%	0.007%
7	700	0.060%	0.001%	0.000%	0.006%
8	800	0.047%	0.001%	0.000%	0.007%
9	900	0.035%	0.000%	0.000%	0.009%
10	1000	0.028%	0.000%	0.000%	0.010%
11	1100	0.021%	0.000%	0.000%	0.011%
12	1200	0.018%	0.000%	0.000%	0.014%
13	1300	0.015%	0.000%	0.000%	0.017%
14	1400	0.012%	0.000%	0.000%	0.020%
15	1500	0.010%	0.000%	0.000%	0.024%
16	1600	0.008%	0.000%	0.000%	0.030%
17	1700	0.007%	0.000%	0.000%	0.038%
18	1800	0.006%	0.000%	0.000%	0.045%
19	1900	0.006%	0.000%	0.000%	0.054%
20	2000	**0.005%**	0.000%	0.000%	0.061%

4.4.2 Chip Offset Comparison

Received signal is down sampled to chip rate with different offset positions, i.e., 0 chip, 1/4 chip, and 1/2 chip offset w.r.t the peak sampling point of the matched filter output. Downsampling is performed directly after the matched filtering in case of FFT equalizer and is done after the different delay elements of RAKE fingers in case of GRAKE equalizer.

BER performance results for the two equalization methods for target BER of 10%, 1%, and 0.1% are shown below with different channel models used.

- **Propagation channel:** ***"Single Path*** *(non-time selective)"*

  FFT Simulation Parameters: N_{FFT}=2048, λ_h = 1/200, λ_σ = 1/100, optimum value for ε, and channel estimation despreaders = 31.

  G-RAKE Simulation Parameters: no_fingers = 9, λ_h = 1/100, λ_{R_n} = 1/200

Simulation Length: 1000 WCDMA slots

Table 4.4: Chip Offset Comparison: Single Path Channel

Chip Offset	Target BER	FFT				GRAKE
		IorIoc [dB]	SIR_l	SIR_c	SIR_r	IorIoc [dB]
0 chip	10%	1.03	0.001	32.9	0.001	1.14
	1%	6.30	0.001	108.6	0.001	6.31
	0.1%	8.78	0.001	194.3	0.001	8.75
1/4 chip	10%	1.35	0.006	33.2	0.007	1.09
	1%	6.60	0.002	107.9	0.002	6.30
	0.1%	9.05	0.002	192.8	0.002	8.69
1/2 chip	10%	2.02	0.133	33.4	0.133	1.08
	1%	8.24	0.063	115.2	0.063	6.35
	0.1%	12.38	0.037	241.6	0.036	8.75

In the results, alongwith the required IorIoc values, SIR estimate (mean) results are also shown for the FFT method. Using three despreaders, one for main peak as shown in figure 4.9 and two others at 1 chip offset in the left and right position of the main despreader are used. SIR_c shows the SIR estimate using the main despreader, where SIR_l and SIR_r show SIR estimates of the left and right despreader respectively. From the SIR estimate results, it can be noted that SIR values close to zero are observed for the left and right despreaders if the downsampling has been done at 0 chip offset.

The above results show that both the methods have almost the same performance for single path channel only if the downsampling has been performed properly after the matched filtering. Also the GRAKE method is independent of any offset induced by the downsampling, but the FFT method performance is deteriorated with different chip offset positions. Furthermore the FFT method gives the worst performance if the offset is 1/2 chip.

Conclusion:

When a propagation channel is AWGN like, i.e., having very small ($\approx$ zero) delay spread, the timing of the main peak needs to be determined accurately. This can be accomplished by putting despreader on a potential peak and its $\pm 3/4$ chip neighbors. Measuring the estimated SIR values and fitting to the response anticipated for an AWGN channel will locate accurately the peak.

- **Propagation channel: *"Two Path** (non-time selective)**, Delay Spread = 0.75 chip"***

For all the two path channel models, the following simulation parameters are used:

FFT Simulation Parameters: N_{FFT} = 2048, λ_h = 1/200, λ_σ = 1/100, optimum value for ε, channel estimation despreaders = 15+delay_spread+15.

G-RAKE Simulation Parameters: finger spacing 'τ' = 3/4, λ_h = 1/100, λ_{R_n} = 1/200, no_fingers = (15+delay_spread+15) / τ

Simulation Length: 1000 WCDMA slots

Selecting 'ε' for FFT method

Table 4.5 shows the simulation results of FFT equalizer using **IorIoc = 6 dB** and different values of $\boldsymbol{\varepsilon}$. Propagation channel used is two path (non-fading channel) with delay spread = 0.75 chip. These results show that optimum value of $\boldsymbol{\varepsilon}$ is needed for the FFT equalizer to minimize the BER at the required IorIoc.

Table 4.5: FFT equalizer BER vs $\boldsymbol{\varepsilon}$, IorIoc = 6 dB, two path channel 'ds' = 0.75 chip

Sr. #	1 / ε	BER vs Chip Offset		
		0 chip	1/4 chip	1/2 chip
1	5	3.12%	2.21%	2.33%
2	10	2.60%	1.69%	1.78%
3	15	2.39%	1.52%	1.60%
4	20	2.24%	1.41%	1.47%
5	25	2.19%	1.33%	1.34%
6	30	2.13%	**1.31%**	**1.34%**
7	35	2.08%	1.31%	1.37%
8	40	**2.07%**	1.32%	1.37%
9	45	2.09%	1.31%	1.33%
10	50	2.11%	1.32%	1.34%
11	55	2.14%	1.35%	1.34%
12	60	2.14%	1.30%	1.37%
13	65	2.18%	1.36%	1.42%
14	70	2.19%	1.36%	1.40%
15	75	2.22%	1.33%	1.46%
16	80	2.30%	1.41%	1.43%
17	85	2.23%	1.39%	1.38%
18	90	2.21%	1.45%	1.44%
19	95	2.34%	1.42%	1.42%
20	100	2.35%	1.44%	1.44%

Simulation results for the target BER of 10%, 1%, and 0.1% using two path channel model with delay spread = 0.75 chip are given in table 4.6.

Table 4.6: Chip Offset Comparison: Two Path Channel 'ds' = 0.75 Chip

Chip Offset	Target BER	FFT				GRAKE
		IorIoc [dB]	SIR_l	SIR_c	SIR_r	IorIoc [dB]
0 chip	10%	0.97	0.727	33.0	0.714	1.02
	1%	7.59	0.228	120.7	0.223	6.65
	0.1%	11.13	0.079	230.7	0.077	9.42
1/4 chip	10%	0.62	0.373	33.6	0.368	1.06
	1%	6.38	0.084	110.1	0.083	6.71
	0.1%	9.13	0.041	196.8	0.041	9.30
1/2 chip	10%	0.60	0.427	32.3	0.428	1.01
	1%	6.42	0.073	113.0	0.069	6.64
	0.1%	9.21	0.066	202.8	0.065	9.37

These results show that the GRAKE equalizer has consistent performance with the three different offset positions in downsampling. For the FFT equalizer, downsampling at offset = 1/4 or 1/2 gives the same performance and is also better than the case when offset = 0. The FFT equalizer's performance for these two cases, i.e., offset = 1/2 & 1/4 is also better than the GRAKE equalizer's performance.

In FFT equalizer, for offset = 0, all the chip samples of the received signal experience more interference from the second path as compared to the case when offset = 1/4 is used. That is why we have observed better performance with chip offset = 1/4 with FFT equalizer. And for the case when offset = 1/2 is used, the second path appears to be stronger than the first path in the channel estimates; while the interference intensity remains the same as with offset = 1/4 was observed.

Table 4.7: FFT equalizer BER results at different offset positions using IorIoc = 8 dB

Chip Offset	BER
0	0.81%
1/4	0.35%
1/2	0.34%
1	0.80%
5/4	0.35%

Conclusion:

For non-AWGN like channels (having small but non-zero delay spread), it is not obvious that alignment with one of the peaks gives the best BER results. Possible solutions involve computing two equalizer solutions for different offsets and measure SIR or time multiplex the equalizer with different offsets and selecting the best one. In the latter solution, we periodically would have to check different offsets to know which offset is optimal.

- **Propagation channel:** ***"Two Path*** *(non-time selective)****, Delay Spread = 1 chip"***

Simulation results for the target BER of 10%, 1%, and 0.1% for the two methods (FFT and GRAKE) are given below:

Table 4.8: Chip Offset Comparison: Two Path Channel 'ds' = 1 Chip

Chip Offset	Target BER	FFT				GRAKE
		IorIoc [dB]	SIR_l	SIR_c	SIR_r	IorIoc [dB]
0 chip	10%	3.08	1.697	31.5	1.675	3.70
	1%	12.93	0.292	133.8	0.286	13.45
	0.1%	20.09	0.101	321.8	0.102	21.45
1/4 chip	10%	3.23	1.463	32.9	1.478	3.84
	1%	13.67	0.357	142.1	0.366	13.31
	0.1%	22.58	0.055	342.4	0.051	20.69
1/2 chip	10%	3.25	1.782	33.1	1.822	3.76
	1%	14.95	0.550	150.1	0.542	13.52
	0.1%	28.0	0.089	368.0	0.089	21.20

The above results for two path channel with delay spread = 1 chip show that the BER performance for FFT method is superior to the GRAKE method, if proper downsampling has been done before the equalization. Also comparable performance is observed if the downsampling is performed at offset = 1/4 chip. The FFT method's performance becomes worse than the GRAKE performance if offset = 1/2 is used. These results also show that the FFT method performs better than the GRAKE in all the cases if the target BER is 10%.

- **Propagation channel: *"Two Path** (non-fading)**, Delay Spread = 4.5 chip"***

Simulation results for two path channel with delay spread = 4.5 chip are shown in table 4.9.

Table 4.9: Chip Offset Comparison: Two Path Channel 'ds' = 4.5 Chip

Chip Offset	Target BER	FFT				GRAKE
		IorIoc [dB]	SIR_l	SIR_c	SIR_r	IorIoc [dB]
0 chip	10%	3.01	0.005	33.5	0.005	3.50
	1%	11.28	0.007	120.7	0.006	13.09
	0.1%	16.64	0.004	238.7	0.004	-
1/4 chip	10%	2.89	0.014	34.0	0.015	3.52
	1%	11.08	0.009	117.0	0.010	13.27
	0.1%	16.53	0.004	240.9	0.004	-
1/2 chip	10%	3.07	0.006	32.9	0.005	3.55
	1%	11.24	0.005	118.2	0.005	13.20
	0.1%	16.60	0.003	232.4	0.003	-

The above results show that no significant performance degradation is observed at different chip offset positions in the downsampling for the two methods and consistent results are obtained. Also, the results illustrate that the FFT method has performed much better than the GRAKE equalizer for the channel model used. Furthermore, based on the above results it is clear that to achieve a target BER of 0.1%. FFT method requires about an IorIoc = 16.6 dB. On the other hand, IorIoc value more than 28 dB is required for the GRAKE equalizer.

- **Propagation channel: *"Two Path* (non-fading)*, Delay Spread = 5 chip"***

Table 4.10: Chip Offset Comparison: Two Path Channel 'ds' = 5 Chip

Chip Offset	Target BER	FFT				GRAKE
		IorIoc [dB]	SIR_l	SIR_c	SIR_r	IorIoc [dB]
0 chip	10%	3.21	0.001	33.0	0.001	3.98
	1%	11.89	0.002	118.2	0.002	14.18
	0.1%	17.22	0.001	237.7	0.001	-
1/4 chip	10%	3.46	0.008	32.8	0.007	4.01
	1%	12.32	0.004	118.4	0.003	14.62
	0.1%	17.65	0.003	223.7	0.003	-
1/2 chip	10%	3.92	0.042	33.5	0.042	3.92
	1%	13.91	0.031	121.9	0.030	14.31
	0.1%	21.16	0.022	244.9	0.021	-

For a delay spread = 5 chip, simulation results using the FFT method and NP-GRAKE method are presented above in table 4.10. These results illustrate that the FFT equalizer can provide better performance than the GRAKE equalizer. Again, it is shown in the results that the best performance for FFT equalizer is only achieved if the downsampling has been performed appropriately at the receiver after the matched filtering.

4.4.3 Frequency Error Comparison

If the clocks of UE and Node B are not synchronized, then there will be a phase offset generated in the UE clock. This residual phase offset accumulates with time and causes phase rotation in the received signal. To simulate this problem, and to observe the performance of the time domain (NP-GRAKE) and frequency domain (FFT) equalizers, simulations are performed for different frequency errors = 5, 10, 15, and 20 Hz. BER performance for the case with frequency error = 0 Hz is also shown for reference.

For the case of frequency errors at the UE, fast filtering, i.e., higher value of λ_h is required for the filtered channel estimate as used in (3.11) and (3.23). Multiple simulations are performed and on the basis of obtained results, it is found that λ_h = 1/40 (i.e., about 4 WCDMA slots) could be an appropriate value to filter the channel estimates, in case of frequency errors. Other simulation parameters used in the simulations are the same. Simulations results for different channel models using λ_h = 1/40 and λ_h = 1/200 are given below for the above mentioned set of frequency errors.

- **Propagation channel: *"Single Path** (non-fading)**, Offset = 0 chip"***

Table 4.11: Frequency Error Comparison: Single Path Channel, Offset = 0 Chip

Frequency Errors	**Target BER**	λ_h = 1/200		λ_h = 1/40	
		FFT	**GRAKE**	**FFT**	**GRAKE**
		IorIoc [dB]	**IorIoc [dB]**	**IorIoc [dB]**	**IorIoc [dB]**
0 Hz	10%	1.06	1.11	1.18	1.13
	1%	6.29	6.27	6.63	6.32
	0.1%	8.84	8.76	9.36	8.69
5 Hz	10%	3.33	3.84	1.32	1.23
	1%	10.62	13.75	6.74	6.52
	0.1%	13.80	-	9.56	9.08
10 Hz	10%	15.06	-	1.58	1.47
	1%	-	-	7.32	7.11
	0.1%	-	-	10.44	10.05
20 Hz	10%	-	-	2.54	2.72
	1%	-	-	9.39	10.43
	0.1%	-	-	13.04	18.45

For the given single path channel at offset = 0 chip, simulation results show that both the methods can perform sufficiently well up till 10 Hz with a slightly better performance results from GRAKE as compared to the FFT method. For 20 Hz case, FFT method performs better than the GRAKE method. Also the FFT method works in a reasonable IorIoc limits for a target BER of 0.1% while the required IorIoc becomes too high for the GRAKE method.

- **Propagation channel:** ***"Single Path*** *(non-time selective)****, Offset = 1/2 chip"***

Observed results for different frequency errors using the single path channel, and downsampling performed at chip offset = 1/2 chip are shown below:

Table 4.12: Frequency Error Comparison: Single Path Channel, Offset = 1/2 Chip

Frequency Errors	**Target BER**	λ_h = 1/200		λ_h = 1/40	
		FFT	**GRAKE**	**FFT**	**GRAKE**
		IorIoc [dB]	**IorIoc [dB]**	**IorIoc [dB]**	**IorIoc [dB]**
0 Hz	10%	2.08	1.11	2.14	1.14
	1%	8.20	6.33	8.51	6.26
	0.1%	12.30	8.77	13.08	8.80
5 Hz	10%	4.54	3.90	2.22	1.26
	1%	13.77	13.88	8.69	6.45
	0.1%	21.31	-	13.64	8.93
10 Hz	10%	18.92	-	2.47	1.50
	1%	-	-	9.49	7.14
	0.1%	-	-	15.29	10.03
20 Hz	10%	-	-	3.49	2.64
	1%	-	-	12.16	10.47
	0.1%	-	-	19.84	18.70

These results show that the performance of the GRAKE equalizer has not been changed while the FFT equalizer's performance has become worse because the downsampling is now performed at time offset = 1/2 chip. In these results the GRAKE performance is always better than the FFT method, yet the performance of both the methods is robust to frequency errors up to 10 Hz.

- **Propagation channel: *"Two Path** (non-fading)**, Delay Spread = 5 chip, Offset = 0 chip"***

Table 4.13: Frequency Error Comparison: Two Path Channel 'ds' = 5 Chip, Offset = 0 Chip

Frequency Errors	**Target BER**	λ_h = 1/200		λ_h = 1/40	
		FFT	**GRAKE**	**FFT**	**GRAKE**
		IorIoc [dB]	**IorIoc [dB]**	**IorIoc [dB]**	**IorIoc [dB]**
0 Hz	10%	3.32	4.01	3.51	4.08
	1%	12.02	14.52	12.68	14.59
	0.1%	17.49	-	18.98	-
5 Hz	10%	6.57	24.88	3.59	4.30
	1%	19.88	-	12.94	15.40
	0.1%	-	-	19.66	-
10 Hz	10%	-	-	3.86	4.94
	1%	-	-	13.85	23.57
	0.1%	-	-	21.30	-
20 Hz	10%	-	-	5.21	10.76
	1%	-	-	18.23	-
	0.1%	-	-	-	-

For two path channel with delay spread = 5 chip, simulations results of the two methods are shown above in table 4.13. These results show that the FFT method has better results than the NP-GRAKE equalizer. Also the FFT method performs suitably well for frequency errors up till 10 Hz for the given channel conditions.

Conclusion:

FFT method is robust for frequency errors up to 10Hz, similarly to G-RAKE.

4.4.4 Colored Noise Comparison

The performance of the two equalization schemes (NP-GRAKE and FFT) has been compared for the colored noise scenario, i.e., another base station (Node B) causing interference in the WCDMA signal from the desired base station (Node B). No Additive White Gaussian Noise (AWGN) is added and only pure colored noise is used as interference in the simulations.

Simulation results of the two equalizers for a target BER of 10%, 1%, and 0.1% are shown below by using different channel models in the simulations.

Table 4.14: Colored Noise Comparison

Target BER	**Single Path, Offset 0**		**Single Path, Offset 2**		**Two Path (ds = 5 chip), Offset 0**	
	FFT	**GRAKE**	**FFT**	**GRAKE**	**FFT**	**GRAKE**
	IorIoc [dB]	**IorIoc [dB]**	**IorIoc [dB]**	**IorIoc [dB]**	**IorIoc [dB]**	**IorIoc [dB]**
10%	0.21	0.45	1.21	0.48	2.98	2.33
1%	7.38	7.49	8.39	7.60	10.26	11.49
0.1%	10.83	10.86	11.84	10.91	14.32	-

The above results show that FFT equalizer performs better than the GRAKE for single path at offset = 0 as well as for the two path channel. Also it is important to note that for two path channel with ds = 5 chip, a target BER of 0.1% using GRAKE method requires more than 28 dB of IorIoc while the FFT method requires only IorIoc = 14.32 dB, whereas, the GRAKE method requires lesser IorIoc than FFT for a target BER of 10%.

Conclusion:

FFT method is as robust as the G-RAKE method to colored noise, even though the used FFT method does not model the colored noise in its algorithm.

4.4.5 Analog-to-Digital Converter Comparison

Analog-to-Digital converter (A/D) is used before the Rx filter to convert the floating point signal into 8-bits, 10-bits, or 12-bits signed int values w.r.t the A/D used. Simulation results are given below for the two equalization methods (NP-GRAKE and FFT). Also for comparison to the case where no A/D is used, simulation results are also shown. In the simulation results, value of the A/D constant (K) is also shown that is used in the simulations to scale the signal for integer representation.

- Propagation channel ***"Single Path** (non-fading)**, Chip Offset = 0 chip"***

Table 4.15: A/D Conversion Comparison: Single Path, Offset = 0 Chip

Target BER	**No A/D**		**8-bit** (K=50)		**10-bit** (K=150)		**12-bit** (K=600)	
	FFT	**GRAKE**	**FFT**	**GRAKE**	**FFT**	**GRAKE**	**FFT**	**GRAKE**
	IorIoc [dB]	**IorIoc [dB]**	**IorIoc [dB]**	**IorIoc [dB]**	**IorIoc [dB]**	**IorIoc [dB]**	**IorIoc [dB]**	**IorIoc [dB]**
10%	1.03	1.14	1.04	1.12	1.04	1.11	1.09	1.12
1%	6.30	6.31	6.27	6.32	6.34	6.30	6.32	6.33
0.1%	8.78	8.75	8.79	8.72	8.81	8.66	8.81	8.83

- Propagation channel ***"Single Path** (non-fading)**, Chip Offset = 1/2 chip"***

Table 4.16: A/D Conversion Comparison: Single Path, Offset = 1/2 Chip

Target BER	**No A/D**		**8-bit** (K=50)		**10-bit** (K=150)		**12-bit** (K=600)	
	FFT	**GRAKE**	**FFT**	**GRAKE**	**FFT**	**GRAKE**	**FFT**	**GRAKE**
	IorIoc [dB]	**IorIoc [dB]**	**IorIoc [dB]**	**IorIoc [dB]**	**IorIoc [dB]**	**IorIoc [dB]**	**IorIoc [dB]**	**IorIoc [dB]**
10%	2.02	1.08	2.11	1.09	2.05	1.12	2.02	1.10
1%	8.24	6.35	8.22	6.30	8.27	6.31	8.17	6.34
0.1%	12.38	8.75	12.37	8.72	12.34	8.72	12.03	8.73

- Propagation channel ***"Two Path** (non-fading)**, Delay Spread = 5 chip, Chip Offset = 0 chip"***

Table 4.17: A/D Conversion Comparison: Two Path 'ds' = 5 Chip, Offset = 0 Chip

Target BER	**No ADC**		**8-bit** (K=50)		**10-bit** (K=150)		**12-bit** (K=600)	
	FFT	**GRAKE**	**FFT**	**GRAKE**	**FFT**	**GRAKE**	**FFT**	**GRAKE**
	IorIoc [dB]	**IorIoc [dB]**	**IorIoc [dB]**	**IorIoc [dB]**	**IorIoc [dB]**	**IorIoc [dB]**	**IorIoc [dB]**	**IorIoc [dB]**
10%	3.21	3.98	3.31	3.98	3.27	3.98	3.30	3.96
1%	11.89	14.18	11.75	14.50	11.97	14.30	11.94	14.09
0.1%	17.22	-	17.14	-	17.20	-	17.16	-

The above simulation results show that both equalizers can be used with 8-bit implementation. The value of the A/D constant (K) which is used to multiply the input WCDMA signal is also mentioned in the tables for each A/D. From the above simulation results, it can be noted that both equalizers using the same A/D constant for their implementation. For FFT method, w.r.t the A/D constant (K), the value of ***'ε'*** has to be scaled up by the square of A/D constant, i.e., K^2.

4.4.6 Complexity Comparison

4.4.6.1 FFT Equalizer Output Samples

The output from the FFT equalizer *'x'* as shown in figure 4.8 represents the equalized chips after cancelling the channel effect on the WCDMA transmit signal. Total number of chips that can be equalized by the channel cancellation operation depends on the channel profile (delay spread).

For example, using N_{FFT} = 2048, FFT equalizer can perform channel cancellation operation on 2048 chips at one time. In the simulation results it is found that if all the output chips from the FFT equalizer are used for further despreading and data symbol detection, higher BER is observed. But, if we discard some chips in the end out of these 2048 chips, the BER results are improved. To illustrate more about the number of chips that needs to be discarded, simulation results for two path channel model with 'ds' = 5 chip and 70 chip are shown in figure 4.1.

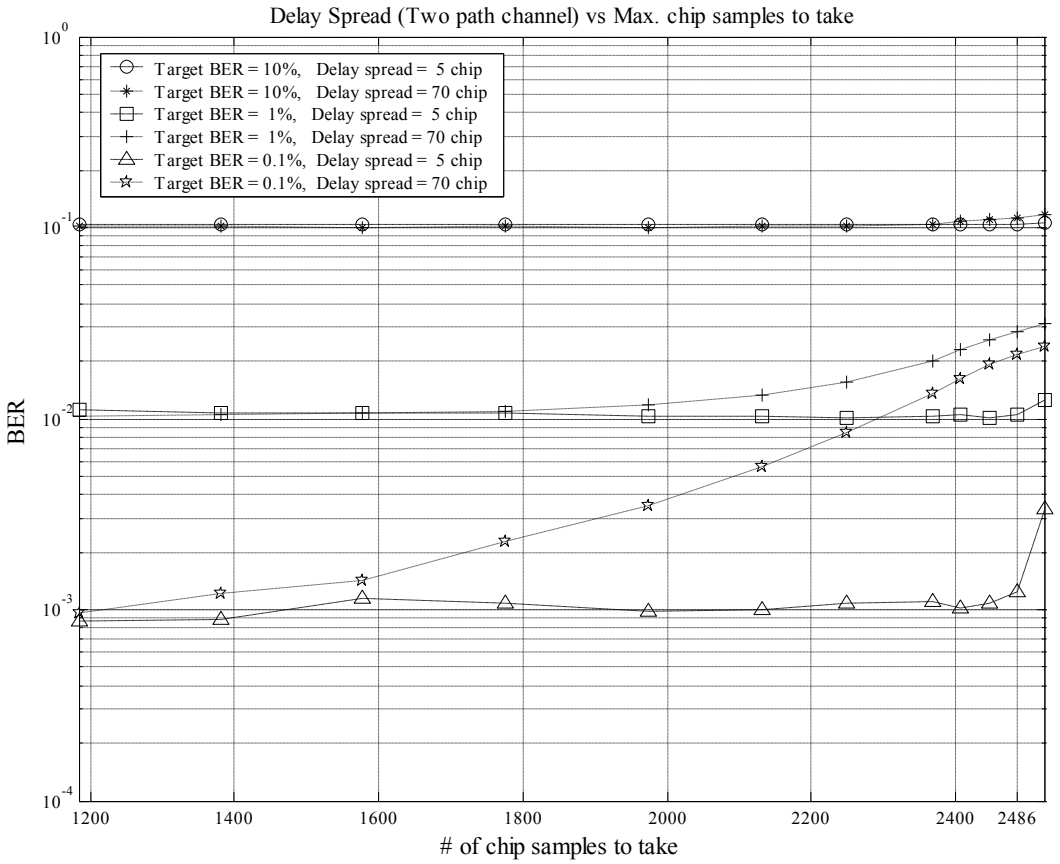

Figure 4.10: FFT Equalizer Output Chip Samples vs Delay Spread

The simulation results show that, for FFT equalizer, the number of chips that are equalized in a WCDMA slot depends on the channel profile (delay spread). Also, the simulations results show that depending on the target BER output chip samples that can be retained are different. For a target BER of 10%, even with a delay spread of 70 chips, all the 2560 output chips can be used for despreading. But for a target BER of 0.1%, and delay spread = 70 chips, number of chip samples to take are about half of the output samples, i.e., 1280 chips. Similarly the above results show that, for a delay spread = 5 chip and target BER of 1% and 0.1%, about 80 chips can be discarded out of 2560 chips while others can be used for despreading and symbol detection.

Now, by using a two path channel with delay spread = 5 chip, in order to process one WCDMA slot complexity comparison for the two equalization schemes is done based on the following computations

- CPICH channel generation
- Equalizer weights generation for NP-GRAKE or FFT method
- FFT and IFFT
- Data demodulation

Assuming that the number of despreaders used for the CPICH channel estimates are same for the two equalization methods. For a two path channel with delay spread = 5 chip, the number of despreaders required for channels estimate = 15+delay_spread+15 = 35 despreaders.

The complexity comparison will be based on the total number of complex operations required for the two equalizers. In general, we will refer to the different arithmetic operations such as multiplication, division, addition, or subtraction as a complex operation.

4.4.6.2 Computations For FFT

Total complex operations required for CPICH channel generation using FFT method is given as

$$35*(256+256+256+1)*10 + (35+35+35)*10 = 270,200$$

where first 256 operations represent the scrambling code multiplications, second 256 operations are for channelization code and third 256 operations are for the summation operation following these multiplications. One division operation is added for CPICH pilot symbol division. Total 35 despreaders are used for channel values estimation. Then the other

operations are used for the filtering operation which is performed on the current channel values and filtered channel values

Total complex operations for an FFT are calculated using the classic Cooley-Tukey method. For a radix-2 algorithm, total complex multiplication required are ~ $(N_{FFT}/2)*\log2(N_{FFT})$ and total complex additions are $(N_{FFT})*\log2(N_{FFT})$, where N_{FFT} is the size of the FFT used [9]. After adding other operations to compute the FFT equalizer numerator and denominator values, using $N_{FFT} = 2048$, total operations required to calculate the FFT equalizer filter are

$$(N_{FFT}+ N_{FFT}/2)*\log2(N_{FFT}) + (N_{FFT}+ N_{FFT}+ N_{FFT}) = 37,888$$

Computations done for taking the FFT of the input signal and the IFFT of the equalized signal are given below

$$(N_{FFT}+ N_{FFT}/2)*\log2(N_{FFT}) + N_{FFT} + (N_{FFT}+ N_{FFT}/2)*\log2(N_{FFT}) = 69,632$$

'M' Equalized chips are taken out based on the decision output from the intelligent block of FFT equalizer. For a delay spread = 5 chip, using $N_{FFT} = 2048$, 'M' = 1984 chips out of 2048 can be retained after equalization. The computations required to detect the data symbols using the descrambling and despreading operations are then

$$M+M+M = 5,952$$

4.4.6.3 Computations for NP-GRAKE

Total complex operations required for CPICH channel generation using NP-GRAKE method are given below, which are the same as for the FFT method

$$35*(256+256+256+1)*10 + (35+35+35)*10 = 270,200$$

The computations required for calculating the noise covariance matrix and further the matrix inversion are determined using the Cholesky based algorithm [10]. Matrix inversion operation is performed once per WCDMA slot and noise covariance matrix is computed 10 times based on the sample channel estimate values. As the covariance matrix is symmetric, total operations are also divided by 2 in the following expression. By including the filtering operation, the number of computations required to get the equalizer filter weights for NP-GRAKE equalizer are:

$$no\_fing^3 / 3 + 2*no\_fing^2 + (no\_fing^2+no\_fing^2+no\_fing^2+no\_fing^2)*(10/2) = 41,242$$

The received signal received at different rake fingers is given the associated weight and the outputs are then combined (MRC). Total complex computations per received data symbol are then:

35*(2560+2560+2560) + (35+35)*80 = 274,400

A complexity comparison for the two equalizers based on the above mentioned results is given in table 4.34.

FFT method total computations = 383,672

G-RAKE method total computations = 585,842

Table 4.18: Complexity Comparison between FFT and G-RAKE

Equalizer method	**Total complex operations required / data symbol**
NP-GRAKE	3,662
FFT	3,094

4.4.7 ITU-Pedestrian B Channel Comparison

For the two equalizers, FFT and NP-GRAKE, simulation results for ITU Pedestrian-B channel (speed = 3km/hr) without AWGN are shown in Figure 4.2. Simulation parameters used are

FFT Simulation Parameters: N_{FFT} = 2048, λ_h = 1/30, ε = 1/50,
channel estimation despreaders = 15+delay_spread+15

G-RAKE Simulation Parameters: finger spacing 'τ' = 3/4, λ_h = 1/30, λ_{R_n} = 1/160,
no_fingers = (15+delay_spread+15) / τ

Simulation Length: 30,000 slots

Using different EcIor values, BER results are plotted for the two equalizers. Where CPICH always uses the same power and power values assigned to the other users are updated corresponding to the EcIor, such that total power is always one.

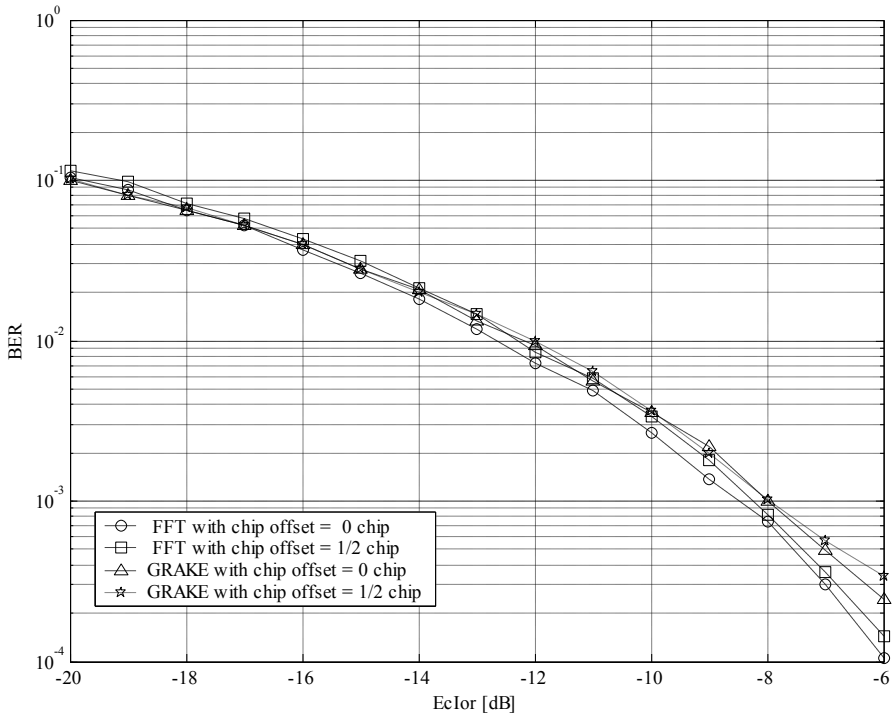

Figure 4.11: BER vs EcIor for FFT and GRAKE equalizer using ITU-PB3 Channel without AWGN

From the obtained results, it is observed that the FFT equalizer with offset = 0 chip always perform better than the GRAKE equalizer. Also the FFT equalizer with offset = 1/2 chip

performs better than the GRAKE equalizer if the desired user have more power assigned. From the results it can be noted that if EcIor is in the range of -12 to -6 dB, then the FFT equalizer is better than the G-RAKE equalizer even if the chip offset = 1/2 chip.

Chapter 5

5 Conclusion

In this thesis, we have investigated two equalization schemes for WCDMA. One is time domain equalization using ML-based Non-parametric G-RAKE method and the other is frequency domain equalization using FFT method. A simulator is made in IT++ and un-coded BER results are used to compare the performance of these two equalizers.

BER performance results for different time offset (0, ¼, ½ chip) received signals are compared. From the observed results, it is found that the performance of FFT based equalizer is better than the G-RAKE equalizer for large delay spread channels. Also, the FFT equalizer has comparable performance to the G-RAKE equalizer for small delay spread channels. It is found that, the G-RAKE equalizer performance is not affected by the different time offset received signals, but, the FFT equalizer has varied performance results. For FFT method, the timing of the main peak needs to be determined accurately for small delay spread channels; and for larger delay spread channels, two equalizer solution might be required by measuring the SIR estimate for two different offsets and selecting the one with highest SIR estimate.

The performance of the two equalizer methods is also compared for different frequency errors generated at the UE. From the obtained results, it is found that both the equalizers are robust to frequency errors at UE, up-to 10 Hz. Simulation results for colored noise (interference from another Node B) show that the FFT equalizer is as robust to colored noise as the G-RAKE method even though the used FFT method does not model colored noise in its algorithm. Also, for analog-to-digital conversion, quantization issues are observed for different fixed point implementations and it is concluded that the FFT method can be used with 8-bit ADC implementation. Total complex operations required per data symbol for FFT and G-RAKE method are determined and it is found that the computations required for FFT method are lesser as compared to the G-RAKE method.

Also, in this thesis, a comparison is shown between FFT and G-RAKE method using ITU-Pedestrian B channel with speed = 3km/hr and frequency = 2.0 GHz. Simulations are

performed using different EcIor values and without AWGN. From the observed results, it is found that the FFT method has better performance than the G-RAKE equalizer for fading and multi-path channel conditions.

In the simulation results it is also observed that, for FFT equalizer, the number of chips output from the equalizer depend on the delay spread. For small delay spread channels almost all the chips in the FFT window are equalized but for medium to larger delay spread channels, lesser chips can be retained at the equalizer output for subsequent despreading and data symbol detection.

Future studies can be performed to optimally place the FFT grid on the input signal to get higher throughput with minimum BER. In the future work, FFT equalizer can be implemented with fixed point implementation for propagation channels with higher Doppler frequencies. Smaller FFT window size will be required at higher velocities as the propagation channels needs to be constant over an FFT window.

Appendix

A. Parametric Equalizer

Assume c_n is the sent chip sequence, and h is a propagation channel including the effects of R_x and T_x radio filters, then we have

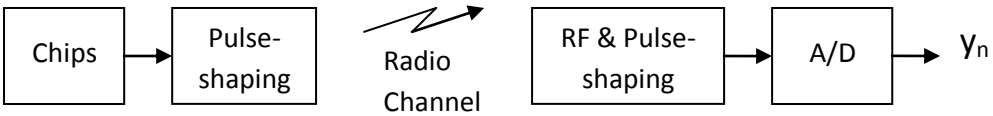

$$y_n = \sum_m h_m c_{n-m}$$

where y_n are sampled at the rate of produced chips c_n. This sampled output is then convolved with a filter g at the receiver and let the final output be denoted by z_n, then

$$z_n = \sum_{\hat{m}} \sum_m h_m c_{n+\hat{m}-m} g_{\hat{m}} = \{k = \hat{m} - m\} = \sum_k \sum_m h_m g_{m+k} c_{n+k}$$
$$\approx \left(\sum_m h_m g_m \right) c_n \quad if \quad \sum h_m g_{m+k} = \delta_k \quad \Leftrightarrow \quad h \otimes g = \vec{e}$$

Here, $\vec{e}$ is a unit vector containing a single 1 and the rest of elements are zero. The task is to find a filter g such that the following expression is minimized

$$\left\| h \otimes g - \vec{e} \right\|^2 + \alpha \left\| g \right\|^2$$

where $\alpha \left\| g \right\|^2$ is a regularization term.

Let $h = \sum_{l=1}^{L} h_l \, z^{-\tau(l)}$ and $g = \sum_{k=1}^{K} g_k \, z^{\rho(k)}$. Then

$$h \otimes g = \sum_{l=1}^{L} \sum_{k=1}^{K} h_l \, g_k \, z^{-\tau(l)+\rho(k)}$$

$$= \sum_{k=1}^{K} \left(\sum_{l=1}^{L} h_l z^{-\tau(l)+\rho(k)} \right) g_k = Hg$$

Here H is a $N \times K$ complex matrix. And $N = -\min \tau + \max \rho + \max \tau - \min \rho$

Let the vector elements represent the delays given by $-\tau(l) + \rho(k), \quad l = 1, \cdots, L$, $k = 1, \cdots, K$ a total of $\leq LK$ elements. Since $-\tau(l) + \rho(k)$ could take on the same value for different pairs (l_1, k_1) (l_2, k_2).

$$H \vec{g} = \vec{e}$$

Minimize with respect to g.

$$\|H\vec{g} - \vec{e}\|^2 + \alpha \|\vec{g}\|^2$$

The second term favors a filter g that smoothes. The factor α determines the amount of smoothing to be used.

Solving for g in $\frac{\partial}{\partial g} \|Hg - e\|^2 + \alpha \|g\|^2 = 0$

$$\Rightarrow \quad g = \left(\left(H^*\right)^t H + \alpha I \right)^{-1} \left(H^*\right)^t e$$, see Appendix B for details.

B. Differentiate $\|Hg-e\|^2$ w.r.t g

Let $g = g + \varepsilon \tilde{g}, \qquad \varepsilon \in \Re$

$(x, y) = x^t y, \qquad x, y$ *column vectors*

Now the directional derivate is

$$\begin{aligned}
&\left(H(g+\varepsilon\tilde{g})-e, H^*\left(g^*+\varepsilon\tilde{g}^*\right)-e^*\right)-\left(Hg-e, H^*g^*-e^*\right)\\
&=\left(Hg-e, H^*g^*-e^*\right)+\left(H\varepsilon\tilde{g}, H^*\left(g^*+\varepsilon\tilde{g}^*\right)-e^*\right)\\
&\quad+\left(Hg-e, H^*\varepsilon\tilde{g}^*\right)-\left(Hg-e, H^*g^*-e^*\right)\\
&=\varepsilon\left(H\tilde{g}, H^*g^*-e^*\right)+\varepsilon\left(Hg-e, H^*\tilde{g}^*\right)+O\left(\varepsilon^2\right)\\
&=\varepsilon\left(\tilde{g}, H^tH^*g^*-H^te^*\right)+\varepsilon\left(\left(H^*\right)^tHg-\left(H^*\right)^te, \tilde{g}^*\right)
\end{aligned}$$

The directional derivate equals (divide above by ε and let $\varepsilon \to 0$)

$$\left(\tilde{g}, H^tH^*g^*-H^te^*\right)+\left(\left(H^*\right)^tHg-\left(H^*\right)^te, \tilde{g}^*\right)$$

Minimize an expression of the type

$$\arg\min_g \alpha_1\|H_1g-e_1\|^2+\alpha_2\|H_2g-e_2\|^2$$

$\Rightarrow$ all directional derivates should equal 0

$$\Rightarrow \quad \left(\tilde{g}, \sum_{i=1}^{2}\alpha_i\left(H_i^tH_i^*g^*-H_i^te_i^*\right)\right)+$$

$$\left(\tilde{g}^*, \sum_{i=1}^{2}\alpha_i\left(\left(H_i^*\right)^tH_ig-\left(H_i^*\right)^te_i\right)\right)=0 \qquad \forall\,\tilde{g}\in C^n$$

$$\Leftrightarrow$$

$$\mathrm{Re}\left(\tilde{g}, f(g)\right)=0 \qquad \forall\,\tilde{g}\in C^n \qquad f(g)=\sum_{i=1}^{2}\alpha_i\left(H_i^tH_i^*g^*-H_i^te_i^*\right)$$

Assume $f(g)\neq 0$, take $\tilde{g}=f(g)^*$ $\Rightarrow$ contradiction.

Thus

$f(g)=0$ at a minimum or

$$\sum_{i=1}^{2} \alpha_i \left(\left(H_i^* \right)^t H_i g - \left(H_i^* \right)^t e_i \right) = 0 \quad \Leftrightarrow$$

$$g = \left(\sum_{i=1}^{2} \alpha_i \left(H_i^* \right)^t H_i \right)^{-1} \left(\sum_{i=1}^{2} \left(H_i^* \right)^t e_i \right)$$

References

[1] Andreas F. Molish, *Wireless Communications*, John Wiley & Sons, England, 2005.

[2] John G. Proakis, *Digital Communications, Fourth Edition*, McGraw-Hill, 2001

[3] Harri Holma and Antti Toskala, *WCDMA for UMTS, Radio Access for Third Generation Mobile Communications, Third Edition*, John Wiley & Sons, England, 2004.

[4] Andrew Richardson, *WCDMA Design Handbook*, Cambridge University Press, 2005.

[5] Viterbi, A., *Principles of Spread Spectrum Communication*, Addison-Wesley, 1997.

[6] Cooper, G. and McGillem, C., *Modern Communication and Spread Spectrum*, McGraw-Hill, 1998.

[7] Ojanperä, T. and Prasad, R., *Wideband CDMA for Third Generation Mobile Communications*, Artech House, 1998.

[8] John B. Anderson, *Digital Transmission Engineering, Second Edition*, IEEE Press, 2005.

[9] P. Duhamel and M. Vetterli, *Fast Fourier Transforms: A Tutorial Review And A State Of The Art,* Signal Processing 19 (1990) pp. 259-299.

[10] Gene H. Golub and Charles F. Van Loan, *Matrix Computations, Third Edition*, The Johns Hopkins University Press, London, 1996.

[11] Yushan Li, Steve McLaughlin, David G. M. Cruickshank, and Xusheng Wei, *Towards Multi-Mode Terminals*, IEEE Vehicular Technology Magazine, vol. 1, pp. 17-24, Dec. 2006.

[12] Ihan Martoyo, Timo Weiss, Fatih Capar, Friedrich K. Jondral, *Low Complexity CDMA Downlink Receiver Based on Frequency Domain Equalization*, IEEE 58th Vehicular Technology Conference, vol. 2(6-9), pp. 987-991, Oct. 2003.

[13] Daniele Lo Iacono, Ettore Messina, Costantino Volpe, Arnaldo Spalvieri, *Serial Block Processing for Multi-Code WCDMA Frequency Domain Equalization*, IEEE Wireless Communications and Networking Conference, vol. 1, pp. 164-170, 2005.

[14] Yushan Li, Steve McLaughlin, David G. M. Cruickshank, *UMTS FDD Frequency Domain Equalization Based on Self Cyclic Reconstruction*, 2005 IEEE International Conference on Communications, vol. 3, pp. 2122-2126, 2005

[15] Brian Eidson, S. Lek Ariyavisitakul, David Falconer, Anader Benyamin-Seeyar, *Frequency Domain Equalization for Single-Carrier Broadband Wireless Systems*, IEEE Communications Magazine, April 2002.

[16] Krauss, T.P., Zoltowski, M.D., Leus, G, *Simple MMSE equalizers for CDMA downlink to restore chip sequence: comparison to zero-forcing and RAKE*, IEEE International Conference on Acoustics, Speech, and Signal Processing, vol. 5, pp. 2865-2868, 2000